UCSF

UC San Francisco Electronic Theses and Dissertations

Title

Left ventricle adaptation to chronic pressure-overload hypertrophy induced by gradual renovascular hypertension in dogs

Permalink

https://escholarship.org/uc/item/1rx7t6m8

Author

Nguyen, Thuan Nghiem Phuoc

Publication Date

1992

Peer reviewed|Thesis/dissertation

LEFT VENTRICULAR ADAPTATION TO CHRONIC PRESSURE-OVERLOAD HYPERTROPHY

INDUCED BY GRADUAL RENOVASCULAR HYPERTENSION IN DOGS

by

THUAN NGHIEM PHUOC NGUYEN

DISSERTATION

Submitted in partial satisfaction of the requirements for the degree of

DOCTOR OF PHILOSOPHY

in

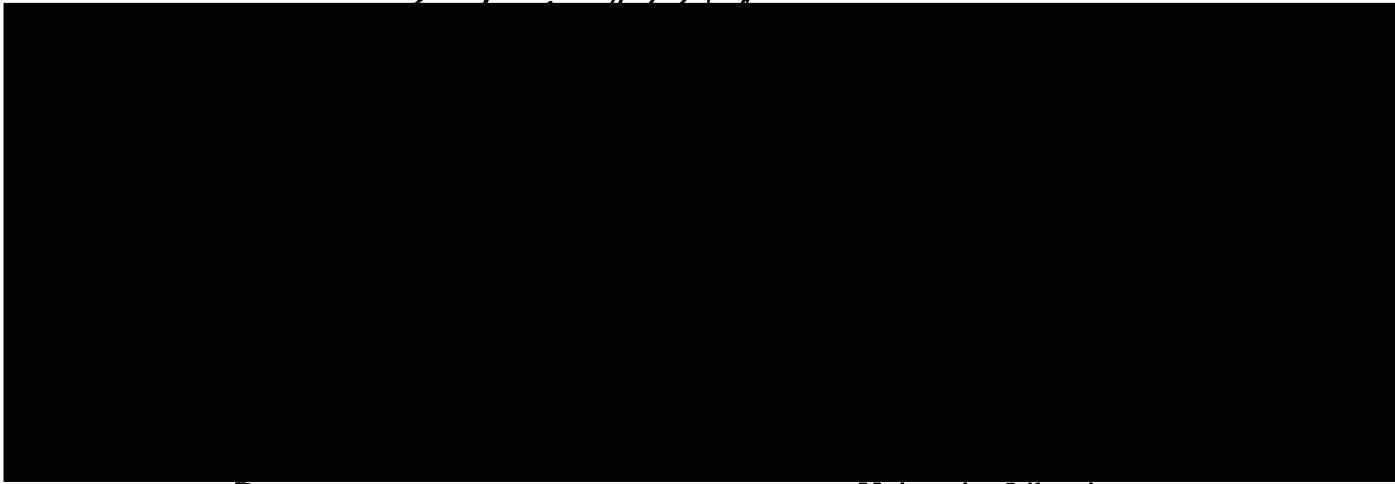BIOENGINEERING

in the

GRADUATE DIVISION

of the

UNIVERSITY OF CALIFORNIA

San Francisco

Date   University Librarian

Degree Conferred: . . /2-3/-92. . . . .

Left Ventricular Adaptation to Chronic Pressure-Overload Hypertrophy

Induced by Gradual Renovascular Hypertension in Dogs

Copyright © (1992)

by

Thuan Nghiem Phuoc Nguyen

Left Ventricular Adaptation to Chronic Pressure-Overload Hypertrophy Induced by Gradual Renovascular Hypertension in Dogs

Thuan Nghiem Phuoc Nguyen

ABSTRACT

The left ventricle hypertrophies in response to chronic pressure overload. This study examines changes in left ventricular (LV) function during the early development of pressure-overload hypertrophy induced by renovascular hypertension, by addressing the questions:

1) Does hypertrophy normalize peak-systolic circumferential wall stress, as is commonly believed?

2) Is increased beta-adrenergic stimulation, wall mass, intrinsic contractility, or a combination of these factors responsible for the improved LV pump function during pressure-overload hypertrophy?

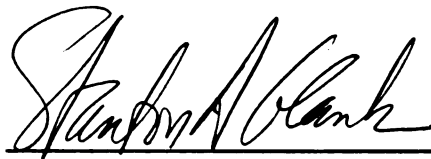3) Does the contraction pattern of the left ventricle change significantly during hypertrophy?

Pressure overload was induced in intact-chest dogs by gradual constriction of one renal artery, and radiopaque markers were implanted in the LV endocardium to measure dimensions. This preparation permits studying gradual changes in cardiac function over time without disrupting the chest, heart, or pericardium. Changes in hemodynamics, LV dimensions, contractility indices, and circumferential wall stress were measured, before and after acute beta-blockade, for 12 weeks.

In contrast to accepted theory, LV systolic circumferential wall stresses decreased significantly over time. End-diastolic circumferential wall stress increased following renal artery constriction, then returned to baseline values as the heart hypertrophied. These results suggest that hypertrophy normalizes end-diastolic, not peak systolic, wall stress.

LV function improved over time in the unblocked state, indicated by increased cardiac output, systolic pressures, stroke work, and E_{max}. Acute beta-blockade reduced stroke work, E_{max}, and dP/dt_{max} relative to the unblocked state, but all still increased significantly over time. dP/dt_{max} and E_{max} did not vary with increases in LV mass, but stroke work was borderline dependent on LV mass. These results suggest that beta-adrenergic stimulation contributes to improved LV pump function, and that the remaining improvements are due to both increased intrinsic contractility and wall mass.

The left ventricle contracts nearly homogeneously and in the same principal directions before and after hypertrophy. Analysis of LV deformation patterns indicated that the LV cross-section is slightly more elliptical after hypertrophy, but the LV contraction pattern does not change significantly despite significant changes in LV dimensions.

Chairman of Committee: Stanton A. Glantz, Ph.D.
Professor of Medicine
University of California San Francisco

ACKNOWLEDGEMENTS

This dissertation project would not have been possible without the logistical help and emotional support of my family, friends, and colleagues.

First, I would like to express my appreciation and gratitude for my dissertation advisor and mentor, Professor Stanton A. Glantz, for giving me lots of practical advice and intellectual inspiration for this project.

I would also like to thank Dr. Antonio Carlos P. Chagas for conducting the pressure-overload hypertrophy experiments, and Mr. James Stoughton for his excellent technical assistance in the lab.

Many thanks to the members of my dissertation committee--Professors Stanton Glantz, Steven Lehman, and David Teitel--for their many constructive suggestions.

I would like to thank my parents for encouraging me to achieve scholastically. Their emotional and financial support over the years have made it possible for me to obtain this Ph.D. degree today.

Special thanks go to Dr. Fred Obermeier, whose constant encouragement and support made it possible for me to complete this dissertation on time.

Thanks also to Dr. Stephen Sizemore and Mr. Franklin Cook for keeping the computers working, to Ms. Mimi Zeiger for her helpful advice on writing style, and to Dr. Fernando Florenzano for performing the volume-overload hypertrophy experiments.

And finally, thanks to all my friends and colleagues in the Bioengineering Graduate Group at the University of California San Francisco and Berkeley Campuses, for making my days in graduate school fun and enriching.

TABLE OF CONTENTS

LIST OF TABLES

LIST OF FIGURES

Chapter 1: Introduction

The left ventricle of the heart grows larger (hypertrophies) in response to two categories of disturbances, pressure overload or volume overload. Pressure overload occurs when arterial pressures are elevated above normal levels (hypertension). Volume overload occurs when either the aortic or the mitral valve develops a leak and allows blood to flow backwards (regurgitation). Pressure and volume overload affect left ventricular (LV) hypertrophy differently. In pressure overload, the LV wall thickness increases while the LV cavity diameter and volume remains constant or decreases slightly (concentric hypertrophy). In contrast, in volume overload, the LV wall thickness remains constant while the LV cavity diameter and volume increase in size (eccentric hypertrophy). Grossman et al. (24) hypothesized that these differences in hypertrophy patterns reflect differences in the changes in wall stress associated with the different loading conditions, based on a study of a select group of human patients.

In volume-overload hypertrophy, Grossman et al. suggested that end-diastolic circumferential wall stress increases after overload is induced, and the left ventricle hypertrophies to decrease end-diastolic wall stress; hypertrophy continues until end-diastolic wall stress returns to normal. This hypothesis has been confirmed for volume-overload hypertrophy induced by aortic regurgitation in dogs (15).

In pressure-overload hypertrophy, Grossman et al. proposed that increased peak-systolic circumferential wall stress stimulates LV hypertrophy and that LV wall thickening decreases peak-systolic wall stress; thickening continues until peak-systolic wall stress returns to normal. This hypothesis is flawed because it does not explain a condition called "inappropriate hypertrophy", in which patients have hypertension and concentric hypertrophy, but <u>subnormal</u> systolic wall stress. Nor does this hypothesis

explain why many hypertensive patients never develop left ventricular hypertrophy despite the pressure overload on their hearts.

The different patterns of systolic wall stress among patients with pressure-overload hypertrophy may be due to the stimulus to hypertension. In a study of perinephritic hypertension in dogs, both end-diastolic and end-systolic wall stresses increase after induction of hypertension, but then decrease back to normal levels by 14 weeks (19,57). These results suggested that hypertrophy could normalize both end-diastolic and end-systolic wall stresses. In contrast, in a study of renovascular hypertension in dogs, end-systolic wall tension did not increase significantly 3 weeks after renal artery constriction; end-diastolic wall tension was not reported (31). These results suggest that renal artery constriction may induce pressure-overload (concentric) hypertrophy in the absence of elevated systolic wall stress, similar to "inappropriate hypertrophy". If systolic wall stress did not increase, could the hypertrophy have been induced by increased end-diastolic stress?

The first goal of this study is to determine whether an increase in end-diastolic (rather than peak-systolic) circumferential wall stress stimulates left ventricular hypertrophy in renovascular hypertension.

Improved LV Pump Function during Pressure-Overload Hypertrophy

Increased left ventricular pump function has been observed in pressure-overloaded hearts during the early development of hypertrophy, before heart failure sets in; the cause of the increased function is not universally agreed upon. Broughton and Korner (7) found that dP/dt_{max} and cardiac index (cardiac output per kilogram of body weight) were significantly increased in hypertrophied hearts from dogs with renovascular hypertension; the increase was attributed to the presence of additional muscle with normal contractility. Ison-Franklin et al. (31) also reported that cardiac output was increased in dogs after 3 weeks of renovascular hypertension, although the

increase was not statistically significant. Sasayama et al. (51) reported increased LV pump function in dogs with pressure-overload hypertrophy induced by chronic aortic constriction. They found increased LV wall shortening velocity and increased systolic wall shortening (indicated by a leftward shift in the relation between LV pressure and diameter) after hypertrophy compared to before hypertrophy. However, because they observed no difference in the relationships between LV wall stress and wall shortening, and between LV wall stress and diameter before and after hypertrophy, they concluded that the hypertrophied hearts had normal inotropic state. Gelpi et al. (18) found that LV wall shortening velocity and dP/dt_{max} increased after hypertrophy induced by perinephritic hypertension, but that these increases were abolished during acute beta-blockade. They concluded that the major mechanism for increased LV pump function was increased sympathetic tone rather than increased wall mass, in contrast to the findings of Broughton and Korner (7), and Sasayama et al (51).

The second goal of this study is to determine whether increased LV pump function, defined by increased dP/dt_{max}, E_{max}, and stroke work, is significantly dependent on increased mass (more muscle fibers in parallel), increased beta-adrenergic stimulation, or some other factor such as increased intrinsic myocardial contractility or ventriculoarterial coupling.

LV Contraction Patterns Before and After Hypertrophy

The contraction of the normal left ventricle can be modeled as a homogeneous deformation--dilation or contraction along three mutually perpendicular principal directions, e.g. base-apex, anterior-posterior, and septum-free wall (25,65). As the left ventricle hypertrophies, its shape and contraction pattern may change. The amount and orientation of dilatation in the end-diastolic shape before and after hypertrophy is unknown. Whether the principal directions of contraction change their orientations after

hypertrophy is unknown as well. Finally, whether pressure and volume overload affect the LV shape and contraction patterns differently is also unknown.

The third goal of this study is to determine whether the left ventricle continues to deform homogeneously, whether it deforms in the same principal directions, and how much its reference shape deforms in each direction.

Organization of Dissertation

In this study of intact-chest dogs, pressure-overload hypertrophy occurred as a result of renovascular hypertension induced by gradual constriction of the left renal artery without disturbing the contralateral kidney and renal artery. Radiopaque markers were implanted in the LV endocardium to measure dimensions. This preparation permits studying gradual changes in cardiac function over time without disrupting the chest, heart, or pericardium. Changes in hemodynamics, LV dimensions, contractility indices, and circumferential wall stress were measured, before and after acute beta-blockade, for 12 weeks. The surgical procedures, measurement methods, and basic statistical analysis are described in Chapter 2.

Chapter 3 reports changes in clinical variables which confirm that the left ventricle hypertrophied over the 12-week study period.

Chapter 4 focuses on the changes in left ventricular pump function during 12 weeks of hypertrophy and describes the multiple linear regression used to analyze these changes.

Chapter 5 reports the changes in circumferential wall stresses over time and their relation to left ventricular wall thickening.

Chapter 6 describes the derivation of left ventricular contraction patterns and compares deformations of hypertrophied hearts to their baseline deformation patterns.

Chapter 7 summarizes the findings of this study and their implications.

Chapter 2: Experimental Methods

Introduction

The left ventricle of the heart hypertrophies in response to increased loading conditions--pressure or volume overload. In this chapter, the basic methods of inducing hypertrophy are reviewed, then the specific methods used in this study are described, from anesthesia and instrumentation to measurements of pressure, volume, and mass, and finally, statistical analysis.

Review of Methods for Inducing Hypertrophy

Pressure-Overload Hypertrophy. Pressure overload occurs when arterial pressures are elevated above normal levels (hypertension). Hypertension has many causes and can be induced experimentally by the following procedures:

1) constriction of the aorta (main artery leading from the heart). Aortic constriction increases resistance to flow, which acutely decreases blood flow to areas of the body downstream from the constriction. In order to maintain flow at pre-constriction levels, the left ventricle must pump at a higher peak pressure.

2) constriction of one renal artery while leaving the aorta undisturbed. Renal artery constriction increases resistance to blood flow into the kidney, and decreases blood pressure inside the kidney. The kidney responds by increasing secretion of renin, which in turn increases plasma levels of angiotensin II and aldosterone. Angiotensin II acutely constricts blood vessels (vasoconstriction) which increases arterial pressures; angiotensin II also permits hypertrophy of cardiac muscle cells (myocytes). Aldosterone increases

5

retention of sodium, which causes increased water retention, which then increases blood volume. Increased blood volume also increases blood pressures. Aldosterone also causes fibrosis of the heart by stimulating the growth and division of fibroblasts (cells which make fibrous connective tissue such as collagen).

3) constriction of an entire kidney, while leaving the renal arteries and aorta undisturbed (perinephritic hypertension). Constriction of the kidney increases intrarenal pressure, which reduces the pressure gradient across the glomeruli. In response to this reduced pressure gradient, arterial pressure outside the kidney is increased, which results in hypertension. Unlike renal artery constriction, however, perinephritic hypertension does not increase plasma renin, angiotensin II or aldosterone, and does not cause fibrosis.

Volume-Overload Hypertrophy. Volume overload occurs when the ventricular volume at end-diastole (part of the cardiac cycle just before contraction) increases above normal levels. Volume overload can be induced experimentally by puncturing the aortic or mitral valve, or by artificially increasing the volume of blood entering the heart from the veins (arteriovenous fistula). Aortic valve puncture causes arterial blood to leak back from the aorta to the left ventricle during diastole (aortic regurgitation), which increases left ventricular (LV) end-diastolic volume. Mitral valve puncture causes blood to leak from the left ventricle back into the left atrium during systole, whereas an arteriovenous fistula allows arterial blood to enter the left atrium from the arteries via the pulmonary veins. Both of these alterations increase blood pressure and volume in the left atrium, which then leads to increased LV end-diastolic volume.

Methods Used in this Study

In this study, pressure-overload hypertrophy was induced by gradual renovascular hypertension. Hypertension was created by constriction of the left renal artery with an ameroid constrictor; the contralateral kidney and renal artery were undisturbed. This method was favored over more invasive methods (aortic constriction, constriction of the entire kidney, or constriction of the renal artery by screw clamps) because it leaves the chest intact and constricts the renal artery gradually--the ameroid constrictor slowly swells over 4 to 6 days (6).

Left ventricular dimensions were also measured without disrupting the chest, by using echocardiography and biplane cineradiography. Markers were implanted in the left ventricle to track specific points on the endocardial surface. Using markers together with cineradiography provides not only dimension data, but also information about contraction patterns over time. The marker procedure was minimally invasive, because the implantation was done via a catheter.

Data were analyzed by multiple linear regression to account for the effects of many independent variables, e.g. heart rate, preload (end-diastolic volume), and afterload (peak systolic pressure), on each dependent variable, e.g. stroke work or dP/dt_{max}. Regression was chosen instead of analysis of variance (ANOVA), because the data varied continuously over time, and this time structure would not be considered in ANOVA.

In this chapter, the surgical procedures and measurement methods are described. More detailed analysis of left ventricular pump function, wall stress, and contraction patterns will be described in Chapters 4, 5, and 6, respectively.

All experimental procedures were approved by the Committee on Animal Research at the University of California, San Francisco.

Anesthesia

Eight dogs weighing 16-23 kg (19±3 [SD]) were premedicated with an intramuscular injection (3 mg/kg) of Innovar-Vet (20 mg of Droperidol and 0.4 mg Fentanyl per ml). Thirty minutes after the premedication, general anesthesia was induced by intravenous injection of Innovar-Vet (1 mg/kg) and pentobarbital (3 mg/kg). The dogs were intubated and artificially ventilated with a mixture of 60% oxygen and 40% nitrous oxide (Fraser Harleke Quantiflex V.M.C. Anesthesia Machine). Respiratory rate and tidal volume were adjusted (Airshields Ventimeter) and intravenous sodium bicarbonate administered as necessary to maintain pCO_2 at 35-45 mmHg, HCO_3 at 20-28 mmol/l, and pH at 7.3-7.4. Arterial pO_2 always exceeded 80 mmHg. Anesthesia was supplemented with 1 mg/kg of Innovar-Vet each hour intramuscularly; this anesthetic combination produces little effect on cardiac function (38).

Implantation of Markers

The dogs were placed supine in an X-ray system with biplane fluoroscopic and cineradiographic capabilities (16 mm, 60 frames/sec). ECG lead II was monitored. The method of implanting markers with a catheter was previously described (10,13,48). Briefly, a MediTech steerable catheter was advanced into the left ventricle through the carotid artery. Seven to eleven radiopaque tantalum markers (1 x 2 mm wire helices) were then implanted in the left ventricular endocardium. At least one marker was implanted in each of the following locations: the aortic valve ring, the apex, and the septal, anterior, posterior, and free (or lateral) walls. At the end of the instrumentation, a NIH 8F catheter was inserted into the left ventricle through the carotid artery and 30 ml of Renografin-76 was injected by hand. Angiograms were then recorded at 60 frames/sec to verify marker positions. The carotid artery was repaired; no data were collected during this session. We waited approximately one week for the

dogs to recover from the implantation procedure before performing the baseline (0 weeks) experiment.

Protocol

Experiments were performed before hypertension (0 weeks) and 1, 4, 8, and 12 weeks after inducing renovascular hypertension. For each experiment, data were recorded in two states: before (unblocked) and during acute beta-blockade induced by propranolol (1 mg/kg).

In each state, data were recorded in the baseline condition and after phenylephrine or nitroprusside was infused to change the afterload. Phenylephrine (10 mg per 500 ml saline) was infused at rates sufficient to produce two to four stable levels of increased systolic blood pressures, the highest of which was at least 30 mmHg above the baseline value. Nitroprusside (50 mg per 500 ml 5% dextrose solution) was infused at rates sufficient to decrease the systolic blood pressure below the baseline level, but never less than 70 mmHg. Phenylephrine and nitroprusside were only used to generate the end-systolic pressure-volume relationship; thus only the parameters E_{max} and V_d reflect the influence of these drugs.

Pressure and Left Ventricular Geometry Data

Using sterile technique, 5F Millar solid-state micromanometers were placed in the left ventricle and the aortic root through femoral arteries. Left ventricular and aortic pressures and the ECG were recorded (29). End-diastole was defined as the time of rapid upstroke in left ventricular pressure. End-systole was defined as the time of maximum ratio of pressure to volume (36). All catheters were introduced by percutaneous puncture via Cordis 6F catheter sheath introducers. The Millar pressure transducers were warmed at 37.5°C for 12 hours before the experiment to minimize drift. To check for drift of the zero point, the readings from the Millar solid-state

micromanometers were periodically compared to readings from fluid filled catheters temporarily placed in the ventricles.

The respirator was turned off at end-expiration and data were recorded for 15 seconds. The heart was filmed in the frontal and lateral projections at 60 frames/sec in biplane alternating mode.

The pressure and film data were synchronized using a cinemark that simultaneously blanked the film and superimposed a pulse on the ECG. The film was projected onto a Talos digitizing tablet, then the marker positions were digitized by hand. The digitized film data were screened for errors by verifying that the coordinates of the marker projections on each of the image intensifiers varied smoothly from frame to frame (27). The resulting data were employed to compute the markers' three-dimensional coordinates (13). The coordinates were used to compute volume (eigenvolume) and to estimate a best-fit ellipsoid for the left ventricular chamber. The ellipsoid was used to compute circumferential wall stress.

Verification of Marker Positions

The dogs were killed 1 to 2 weeks after the 12-week experiment (after an acute study on ventricular interaction (59)) and the hearts were removed and fixed with 10% buffered formalin. The fixed hearts were radiographed to confirm that the marker placement was satisfactory. Finally, the ventricular walls and septum were cut apart and weighed.

Induction of Renovascular Hypertension

To induce renovascular hypertension immediately after the baseline data collection (0 weeks) the left kidney was exposed through a flank incision, and a clay-filled ameroid constrictor (Three Points Products, Montreal, Canada) was placed around the renal artery, according to the technique described by Young (71) and Ben

et al. (4). After implantation, the ameroid clay slowly swells as it absorbs fluids and gradually constricts the artery, thus causing renovascular hypertension. During the 4 days after surgery the dogs were treated with penicillin and streptomycin (Combiotic, Pfizer, New York, 3.0 ml/day). No complications occurred from this procedure.

After the dogs were killed, the kidney was exposed to verify that the constrictor was in place on the renal artery.

Echocardiographic Measurements

For echocardiographic measurements, the dog lay on its right side on a sheet of plexiglass that had holes drilled into it for transducer placement. Echocardiograms were recorded by an Irex-188 machine, and were performed according to the technique described and validated by Schiller et al. (53). The quantitative analysis of the echocardiograms was performed on a Diasonics digitizing system using a RMI 412 phantom to calibrate the distance scale.

Left ventricular wall mass was calculated using the truncated ellipsoid model (53). Mean short axis radius of the left ventricle was calculated as

$$r = \sqrt{A_1 / \pi}$$

and mean equatorial thickness of the left ventricle was calculated as

$$h = \sqrt{A_2 / \pi} - r$$

In which A_1 is the area enclosed by the endocardium and A_2 is the area enclosed by the epicardium in the short axis view at the level of the papillary muscle tips.

Validation of Echocardiographic Method:

This technique of estimating mass was validated by regressing postmortem left ventricular wall mass against wall mass determined by echocardiography; excellent agreement was obtained. Figure 1 shows the left ventricular wall mass computed from the two-dimensional echocardiograms for the current study, as well as data collected in normal dogs of varying sizes by Schiller et al.(53) and data collected from dogs following three months of hypertrophy due to chronic volume overload (15). The regression lines relating echocardiographically-determined mass and mass measured at autopsy are not significantly different among these three studies, despite differences in ventricular size, shape and wall mass; the method is remarkably repeatable. The overall regression line has a slope of 1.07±0.07 (not significantly different from 1.00) and an intercept of 3.4±6.3 gm (not significantly different from 0). The overall correlation is 0.97 and the standard error of the estimate is only 6 gm, compared to wall masses of the order of 100 gm. Therefore, we can have a high degree of confidence in the wall masses computed from the two-dimensional echocardiograms, despite and changes in wall thickness or chamber geometry.

Left Ventricular Eigenvolume

To normalize for differences in initial size and shape of the left ventricle between dogs, we used eigenvolume, a method to estimate relative left ventricular volume from the three-dimensional coordinates of the tantalum markers (11,15,25,65). All volume measurements were performed using this marker method and the normalized data were then converted into milliliters. The conversion between eigenvolume, V_E , and volume in ml, V_{ml} , was previously determined to be $V_{ml} = 100\ V_E - 11$ in a group of similar-sized dogs which were instrumented the same way as in this study (11).

12
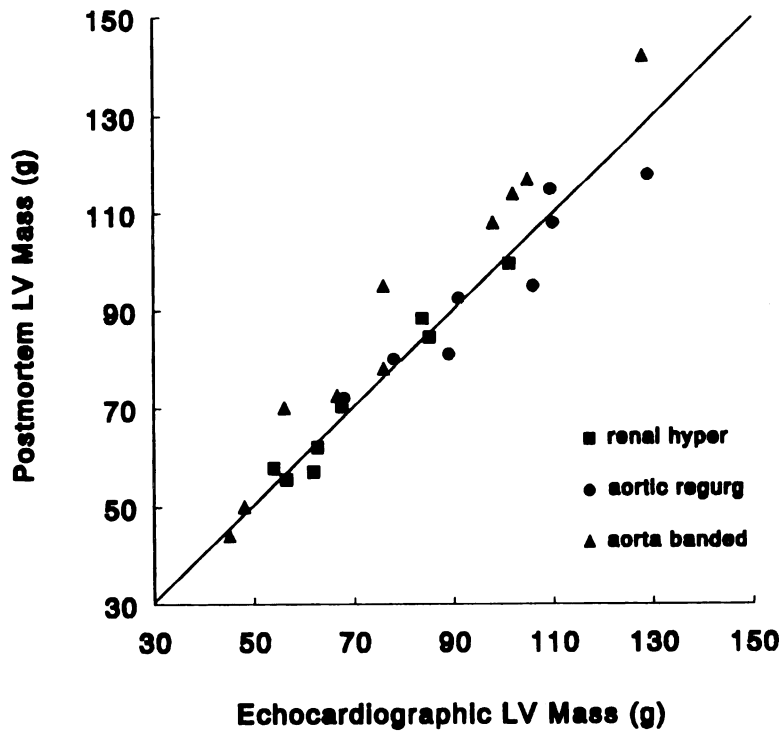
Figure 1. Postmortem left ventricular wall mass is strongly correlated with mass determined by two-dimensional echocardiography in all dogs, regardless of the type of hypertrophy. The regression line has a slope of 1.07±0.07 (SD) (not significantly different from 1.0) and an intercept of 3.4±6.3 g (not significantly different from 0); r = 0.97, SEE = 6 g. Aortic regurgitation data from Florenzano and Glantz (15). Aorta banded data from Schiller et al. (53).

Eigenvolumes were obtained from marker coordinates as follows. The reference size and shape of the left ventricle was considered to be the average three-dimensional coordinates of all the markers in the left ventricle at end-diastole during the baseline experiment done before hypertension. These reference data can be used with the observed three-dimensional marker coordinates at any other time to compute a 3x3 matrix, T, that describes the change in the left ventricle's size and shape relative to this reference size and shape. The determinant of T, known as the eigenvolume, gives a measure of relative left ventricular volume, with the eigenvolume being equal to 1.00 by definition at end-diastole under the reference condition (i.e. baseline end-diastole before hypertension). If the volume of the left ventricle is 80% of the reference end-diastolic volume, the associated eigenvolume will be 0.80. For each dog, all eigenvolumes are referenced to the end-diastolic configuration of the left ventricle before induction of renovascular hypertension (week 0). Thus, because, by definition, the eigenvolumes are all equal to 1.00 in the reference condition, all the left ventricles will have the same starting value of $V_{mi} = 89$ ml at week 0.

General Statistical Analysis

Raw data are summarized as mean ± standard deviation. Parameter estimates from linear and nonlinear regression analysis of the data (described below) are presented as estimate ± standard error of the estimate.

When the variables were plotted against time, curvature was observed in some plots and qualitatively different responses over time between the unblocked and beta-blocked states. To test for the presence of significant curvature, I fitted a quadratic function of time to the data and determined whether the squared term was significant. If this analysis detected significant curvature, I fitted the response with an exponential function of time rather than a linear one. To account for the different responses

between the unblocked and beta-blocked states, I analyzed the data from these states separately. If this separate analysis revealed qualitatively similar responses over time, I performed a single analysis on the combined data. To account for the effects of changes in left ventricular pressure, heart rate, end-diastolic volume, and wall mass on indices of contractility (dP/dt_{max}, dP/dt_{min}, E_{max}, and stroke work), I included these variables in the linear regression equations in Chapter 4. The following subsections describe these analyses in detail.

Testing for Curvature. For all variables, I tested for curvature in the response over time using the multiple linear regression model (20)

$$ y = b_0 + b_t(t-\bar{t}) + b_{t^2}(t-\bar{t})^2 + \sum b_i D_i $$

in which y is the dependent variable of interest (e.g. maximum left ventricular pressure) and t is time after renal artery constriction (in weeks). I centered the time variable on its mean to avoid introducing a structural multicollinearity (20) (from using both t and t^2 in the same regression equation), which could lead to underestimation of the curvature.

$\bar{t} \approx 5$ weeks, depending on the pattern of any missing data. The D_i are 7 dummy variables to permit the 8 different dogs to have different mean responses where

$$ D_i = \begin{cases} 1 \text{ if dog i } (1 \le i \le 7) \\ -1 \text{ if dog 8} \\ 0 \text{ otherwise} \end{cases} $$

The b_i represent the deviation from the overall average value for dog i (i≤7). The deviation of dog 8 from the overall average is $b_8 = -\Sigma b_i$ (i ≠ 8). The between-dogs variability, s_d, is computed as the standard deviation of the b_i. This method of coding the dummy variables is called effects coding (20).

A significant value of b_{t^2} indicates significant curvature in the response of y over time.

Linear Regression Model. If there was no evidence of curvature, I used a linear model to describe the response of variable y over time.

$$y = b_0 + b_t t + \sum b_i D_i$$

In this case, b_0 is the mean value over all dogs and conditions at time zero before renovascular hypertension and b_t is the average change in the dependent variable (y) per unit time.

Exponential Regression Model. If there was evidence of significant curvature and the response appeared to be leveling off, I used an exponential model to describe the change in y over time, because these responses resembled exponential functions and because many biological growth processes follow exponential functions rather than polynomials. I modeled the data using the equation

$$y = b_0 + (b_\infty - b_0)(1 - e^{-t/\tau}) + \sum b_i D_i$$

where b_0 is the value of the dependent variable at time 0 (before renovascular hypertension), b_∞ is the steady state value of the dependent variable and τ is the time constant (in weeks) for the exponential approach to the steady state value. The b_i and D_i are defined as before. The first guesses for the nonlinear regression were selected by looking at a plot of the data.

Because of physiological limits, many variables that increase or decrease over time will eventually reach a plateau. Approximating their responses with an exponential function allows us to estimate when the variable will level off.

Modeling the Effect of Beta-Blockade. The data from the unblocked and beta-blocked states were first analyzed separately using the linear or exponential regression. If the responses before and during blockade were linear, I then determined whether acute beta-blockade caused a parallel shift in the response by adding the dummy variable B to the basic multiple linear regression equation. I also determined whether there was interaction between beta-blockade and time.

The regression equation is

$$y = b_0 + b_B B + b_t t + b_{Bt} Bt + \sum b_i D_i$$

where

$$B = \begin{cases} 0 \text{ if no beta blockade} \\ 1 \text{ if beta blockade} \end{cases}$$

and the product Bt is the variable for interaction. If b_B is significantly different from zero, then there is a systematically higher or lower response over time during acute beta-blockade. b_B is the average change in the dependent variable (y) that accompanies acute beta blockade. If b_{Bt} is significantly different from zero, then the change in y induced by acute beta-blockade is progressively larger or smaller over time.

Statistical Software. Computations were performed using SAS Version 6.06.01. Means and standard deviations were computed with the procedure MEANS. Linear and nonlinear regressions were computed using procedures REG and NLIN, respectively. Centering the time variable was done with procedure STANDARD. Paired t-tests were done with the procedure UNIVARIATE. The various effects were tested for statistical significance by examining the t or the F statistic and its associated p value for each coefficient in the regression equation. In the nonlinear regressions, to

test whether coefficients were significantly different from zero, I used the approximate t value obtained by dividing each coefficient by its asymptotic standard error. A value of $p < 0.05$ was considered statistically significant.

The regression coefficients and their standard errors are reported in the tables, together with the between-dogs variation, s_d , described above and the standard deviation of the mean squared residual error, $s - \sqrt{MS_{res}}$, from the regression analysis. Figures show mean responses, averaged over all 8 dogs, together with the results of the regression analysis. The measures of variability (s_d and s) are reported but not drawn on the figures because the repeated-measures nature of the experimental design does not permit graphical representation of these two distinct components of the variance in the response at each time.

Chapter 3: Confirmation of Left Ventricular Hypertrophy

Introduction

To track the physiological changes that occur during the development of pressure-overload hypertrophy, experiments were performed at 0, 1, 4, 8 and 12 weeks after induction of hypertension by renal artery constriction. Measurements of left ventricular wall thickness, mass, and volume during each experiment confirmed that concentric hypertrophy was occurring.

Clinical Variables

At the end of the 12 weeks, all 8 dogs in this study were healthy and showed no clinical signs of heart failure. There was a borderline significant increase in body weight compared to before renal artery constriction (19 ± 3 (SD) kg at week 0 vs. 20 ± 3 kg at week 12, p=0.052 by paired t-test). The ratio of left ventricular weight divided by body weight, LVW/BW, increased significantly (2.9 ± 0.4 (SD) g/kg at week 0 versus 3.6 ± 0.6 g/kg at week 12, p=0.012 by t-test).

Confirmation of Concentric Hypertrophy

Left ventricular wall mass and thickness increased significantly while volumes either remained constant or decreased, a pattern consistent with concentric hypertrophy in chronic pressure overload (22,23,52).

Left ventricular mass increased linearly by 31% after 12 weeks of renovascular hypertension (from 55 ± 11 to 72 ± 17 g; Figure 2, Table 1). Left ventricular wall thickness increased exponentially by 87% over the same period (from 0.8 ± 0.1 to 1.5 ± 0.2 cm; time constant of 8.2 ± 2.8 weeks; Figure 3). There was no evidence that either wall

19

mass or wall thickness had reached steady state after 12 weeks of renovascular hypertension. The time constant of 8.2 weeks suggests that wall thickness will reach steady state by approximately 40 weeks.

End-diastolic volume did not change significantly over time from a mean of 89 ml at week 0, (Figure 4 and Table 1). End-systolic volume decreased slightly and significantly (from 49 ± 12 to 46 ± 15 ml, Figure 4 and Table 1). As expected, V_d (volume axis intercept of the end-systolic pressure-volume relationship) did not change significantly over time from the initial mean of 8 ± 10 ml (Table 1; computation of V_d is described in Chapter 4).

There was no evidence of right ventricular hypertrophy. The mean postmortem right ventricular wall thickness in dogs with renovascular hypertension, 0.81 ± 0.11 cm, was not significantly different from that of a similar group of normal dogs studied in this laboratory (25), 0.86 ± 0.15 cm (p=0.51 by t-test).

Table 1:   Left Ventricular Wall Mass, Wall Thickness, and Chamber Volume

	0 wk	1 wk	4 wk	8 wk	12 wk	Regression Equation [†]		s_d	s
V_W , g	55 ±11	56 ±13	62 ±14	67 ±16	72 ±17	56 ±1	+ 1.4 t ±0.1***	14	3
h , cm	0.8 ±0.1	0.8 ±0.1	1.1 ±0.2	1.3 ±0.2	1.5 ±0.2	0.8 ±0.0	+ 0.8 ±0.2*** $(1 - e^{-t/8.2})$ ±2.8**	0.9	0.1
Before beta-blockade									
V_{ED}, ml	89 ±0	84 ±8	94 ±5	83 ±11	94 ±26	– [‡]			
V_{ES}, ml	49 ±12	44 ±12	50 ±15	43 ±12	46 ±15	–			
V_d, ml	16 ±17	10 ±15	10 ±14	9 ±13	15 ±13	–			
During beta-blockade									
V_{ED}, ml	98 ±7	89 ±9	98 ±10	92 ±9	97 ±7	90 ±2	+ 6 B ±2 *	6	11
V_{ES}, ml	63 ±17	54 ±17	55 ±17	54 ±14	51 ±13	49 ±1	+ 8 B ±1*** – 0.5 t ±0.2**	14	6
V_d, ml	8 ±10	4 ±14	20 ±14	13 ±10	19 ±13	10 ±2		4	12

Data over time are mean ± standard deviation for 8 dogs.   Parameter estimates are mean ± standard error. B is a dummy variable for acute beta-blockade. B = 0 before blockade and B = 1 during blockade. s_d = between-dogs variation. s = standard deviation of the mean squared residual error.

V_W = echocardiographic LV wall mass, h = LV average wall thickness, V_{ED} = end-diastolic volume, V_{ES} = end-systolic volume, V_d = estimated value of V_{ES} at zero pressure.

[†] Between-dog terms $(\Sigma b_i D_i)$ omitted for clarity
[‡] Refer to pooled regression model during acute beta-blockade.
*   Regression coefficient is significantly different from zero. $P \leq 0.05$; ** $P \leq 0.01$; *** $P \leq 0.001$.
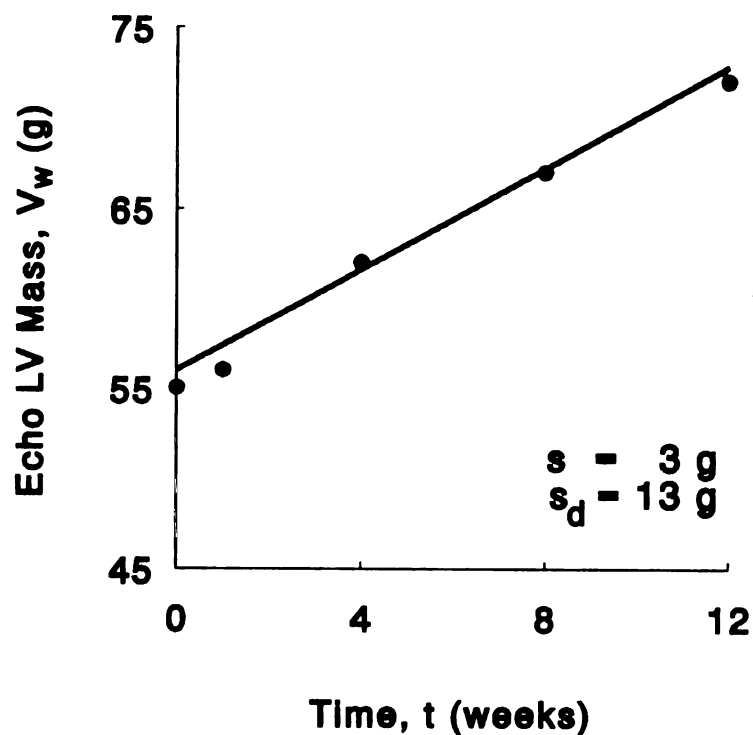
Figure 2. Evidence of hypertrophy during 12 weeks of pressure overload induced by renovascular hypertension. Left ventricular mass increased linearly at a rate of 1.4±0.1 g/week. In this and subsequent figures, each point represents the <u>mean</u> response of all 8 dogs at each time. s_d is the standard deviation of the between-dogs difference and s is the standard deviation of the residual variation, after accounting for the effect of the independent variable and between-dogs differences. If the unblocked and beta-blocked data were analyzed together, then there would be only one set of standard deviations, otherwise there would be two sets.
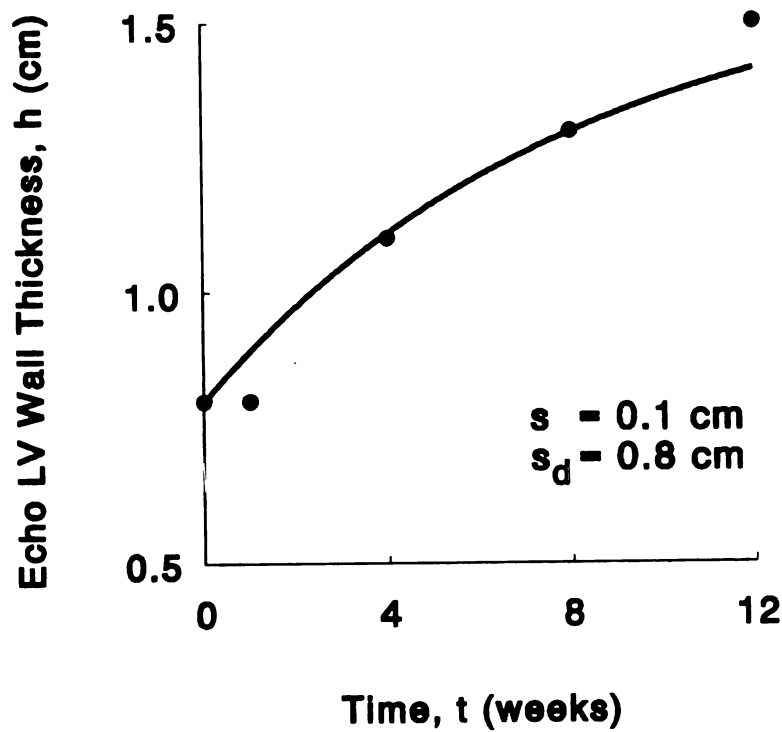
Figure 3. Evidence of pressure-overload hypertrophy. Left ventricular wall thickness increased, consistent with pressure overload induced by renovascular hypertension. The increase was exponential; the time constant was 8.2±2.8 weeks which suggests that the increase will level off at about 40 weeks.
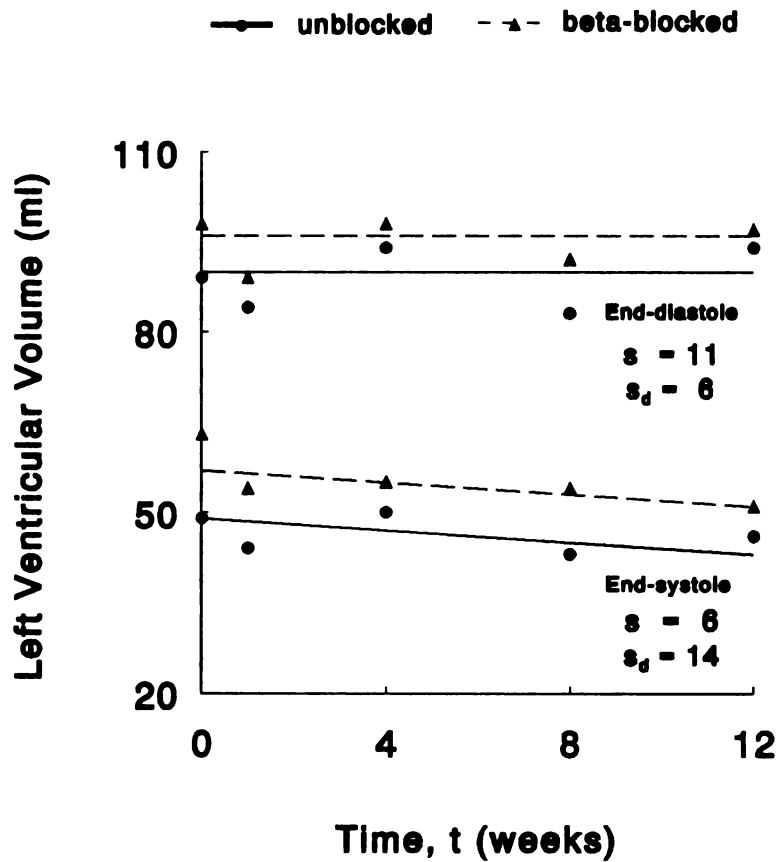
Figure 4. Evidence of concentric hypertrophy. Left ventricular end-diastolic volume remained constant, but end-systolic volume decreased over time, resulting in increased stroke volume. This pattern of constant or slightly decreased volume and increased wall thickness is typical of concentric hypertrophy.

Chapter 4:   Left Ventricular Global Pump Function

Introduction

During early pressure-overload hypertrophy, left ventricular (LV) pump function increases. LV stroke work increases because the ventricle generates more pressure (at a given stroke volume) than before hypertrophy. LV dP/dt_{max} also increases, indicating that the left ventricle can increase pressure more rapidly during isovolumic contraction. In addition, in renovascular hypertension, the stroke volume and heart rate also increase, which result in increased cardiac output. The factors that contribute to this increased pump function are not well understood. Studies of pressure-overload hypertrophy have suggested that either increased wall mass or increased sympathetic tone (beta-adrenergic stimulation) is responsible for improved LV pump function (7,18,51). Changes in intrinsic contractility may also affect pump function, but there is no agreement on whether contractility is normal, increased, or decreased in pressure-overload hypertrophy (51,18,58,60).

To determine how left ventricular pump function adapts to renovascular hypertension, we measured changes in hemodynamics and indices of global LV contractility at 0, 1, 4, 8, and 12 weeks after renal artery constriction. Hemodynamic changes include increased LV and arterial pressures, heart rate, stroke volume, and cardiac output. Indices of contractility are dP/dt_{max} , E_{max} and stroke work.

This study introduces a new approach to analyzing the changes in hemodynamics and indices of contractility; data were analyzed using multiple linear regression models that accounted for the effects of several confounding variables, e.g. end-diastolic volume (preload), LV end-systolic pressure (afterload), heart rate, LV mass, beta-adrenergic stimulation, and ventriculoarterial coupling. Each index of

25

contractility covaries with some of these confounding variables. To determine whether the confounding variables significantly affect each index, it is necessary to include them as independent variables in the regression model.

Definitions of Variables

E_{max} and V_d Computation. The slope, E_{max} , and volume axis intercept, V_d , of the end-systolic pressure-volume relationship were computed from the pressure-volume loops at several different afterloads obtained by infusing phenylephrine and nitroprusside as described by Florenzano and Glantz (15). The end-systolic points were identified by computing the ratio $P(t)/V_E(t)$, locating the maximum value, and then taking the corresponding values of pressure and volume from the pressure-volume loop (Figure 9). This procedure was repeated for data collected at each afterload, and then a linear regression of the resulting (P,V_E) points was computed to obtain E_{max} and V_d . This regression corresponds to the first iteration of the method described by Kono et al. (36), who stated that one iteration is usually sufficient.

Other Computed Variables. Stroke volume, cardiac output, stroke work, and arterial elastance were defined as follows: stroke volume = $SV = V_{ED} - V_{ES}$, cardiac output = SV x HR, stroke work = SV $(P_{MAX} - P_{ED})$, arterial elastance = $E_a = P_{ES} / SV$, where V_{ED} and V_{ES} are end-diastolic and end-systolic volumes, respectively, HR is heart rate, P_{MAX} is maximum left ventricular pressure, and P_{ED} and P_{ES} are left ventricular end-diastolic and end-systolic pressures, respectively. The ratio of E_{max} / E_a , a measure of left ventricular-arterial coupling, was also computed.

Statistical Analysis

Because the indices of contractility (dP/dt_{max}, dP/dt_{min}, E_{max}, and stroke work) also covary with other physiological variables such as left ventricular pressure, heart rate, end-diastolic volume, and wall mass, the effects of these other variables were accounted for in the linear regression model as follows.

E_{max} Normalization.

E_{max} varies between subjects because end-systolic volumes vary in size. One can normalize this variation by dividing left ventricular volume by some reference volume, e.g., V/V_d, before computing the elastance. This method gives $E_{max}V_d$ as the normalized elastance (61,62). In this study, the E_{max} is already normalized this way by the use of eigenvolume.

Normalizing the volume variations does not remove all differences between dogs. For example, there is no reason to expect all the dogs to have exactly the same elastance at baseline (week 0). To account for other intersubject differences, I used effects coding (described above) to allow different dogs to have difference baseline levels of E_{max}.

E_{max} may also vary over time because of increases in left ventricular mass (V_w) in each dog. The variable $E_{max}V_w$ has been used to normalize these mass changes, but I believe that this method is inappropriate in this model of pressure-overload hypertrophy. In principle, $E_{max}V_w$ reduces intersubject variations in the same way as $E_{max}V_d$, because V_w is strongly correlated with V_d in normal hearts. However, in pressure-overload hypertrophy, V_w increases but V_d remains constant, so V_w is less correlated with V_d. Furthermore, simultaneous changes in V_w and intrinsic contractility may occur in the same dog over time. Simply multiplying E_{max} by V_w will not show whether the increases in elastance are due to increased mass or intrinsic contractility.

Instead of using $E_{max}V_w$, I used a modified version of the linear regression approach of Belcher et al.(3). I regressed E_{max} against V_w and included effects coding

for between-dogs differences in baseline E_{max} , that is, $E_{max} = b_0 + b_W V_W + \Sigma b_i D_i$. This regression model will detect any dependence of E_{max} on V_W within subjects, i.e., after taking into account that there are differences in left ventricular baseline size and E_{max} . The results of this regression show that the intrasubject increase in V_W did not change E_{max} significantly in either the unblocked or acutely beta-blocked state, or both states pooled together. Thus, there is no benefit in normalizing E_{max} by V_W in this study.

dP/dt_{max} and dP/dt_{min} Normalization.

dP/dt_{max} and dP/dt_{min} are partially dependent on left ventricular pressure, heart rate, end-diastolic volume, and wall mass. To test whether changes over time in dP/dt_{max} and dP/dt_{min} (as a result of chronic pressure overload) were due to the confounding effects of changes in pressure, heart rate, and volume, I used the linear regression equation

$$y = b_0 + b_{P_{ES}} P_{ES} + b_{HR} HR + b_{V_{ED}} V_{ED} + b_B B + b_t t + b_{Bt} Bt + \sum b_i D_i$$

where y is dP/dt_{max} or dP/dt_{min} , P_{ES} is left ventricular end-systolic pressure, $b_{P_{ES}}$ is the average change in y per unit change in P_{ES}, HR is heart rate, b_{HR} is the average change in y per unit change in heart rate, V_{ED} is end-diastolic volume, and $b_{V_{ED}}$ is the average change in y per unit change in V_{ED} . The variables B, t, Bt and D_i are defined as above. A significant value of b_t indicates that y (i.e., dP/dt_{max} or dP/dt_{min}) is changing over time more than would be expected from concurrent changes in left ventricular pressure, heart rate, and end-diastolic volume.

Because V_W and time were collinear, including both variables in the same regression equation resulted in a sample-based multicollinearity (20) which inflated standard errors. Consequently, I performed a separate regression to test the dependency of y on V_W.

$$y = b_0 + b_{P_{ES}} P_{ES} + b_{HR} HR + b_{V_{ED}} V_{ED} + b_B B + b_{V_W} V_W + \sum b_i D_i$$

Stroke Work Normalization. Stroke work depends on end-diastolic volume (21,46,64). To determine whether stroke work increased over time after accounting for its dependency on end-diastolic volume, I used the equation

$$SW = b_0 + b_{V_{ED}} V_{ED} + b_t t + b_B B + b_{Bt} Bt + \sum b_i D_i$$

where V_{ED} is end-diastolic volume and $b_{V_{ED}}$ is the average change in stroke work per unit change in volume. The other variables are defined as before. To determine whether stroke work increased in association with wall mass (V_W), I replaced the variables for time in the above equation ($b_t t$ and $b_{Bt} Bt$) with $b_{V_W} V_W$.

To determine if stroke work is significantly affected by ventriculoarterial coupling (after accounting on its dependency on end-diastolic volume) (28,41), we used the equation

$$SW = b_0 + b_{V_{ED}} V_{ED} + b_E E + \sum b_i D_i$$

where E is the ratio of E_{max}/E_a , and b_E is the average change in stroke work per unit change in E.

RESULTS

Left Ventricular Function before Beta-blockade

Development of renovascular hypertension was confirmed by significantly increased aortic and left ventricular pressures. Left ventricular pump function was

Improved as shown by significantly increased cardiac output, stroke work and E_{max} during the 12-week study.

Hemodynamics. All pressure variables increased exponentially over time (Table 2-A). Maximum aortic pressure increased by 56% (from 107±7 to 167±6 mmHg; the time constant was 3.0±0.7 weeks). Maximum left ventricular systolic pressure increased by 58% (from 105±7 to 166±7 mmHg; the time constant was 2.9±0.6 weeks). These time constant values indicate that maximum aortic and left ventricular pressures would reach a plateau by about 15 weeks, which is consistent with the observed data.

Aortic diastolic pressure increased by 67% (from 68±12 to 114±6 mmHg). The time constant was 4.1±1.1 weeks, which indicates that aortic diastolic pressure would level off by about 20 weeks (Figure 5).

Left ventricular end-diastolic pressure, P_{ED}, doubled (from 7±3 to 14±5 mmHg; the time constant was 1.5±0.8 weeks). The time constant value indicates that P_{ED} would level out by about 8 weeks, in agreement with the observed data (Figure 6). Because P_{ED} increased rapidly while LV end-diastolic volume remained constant, the results suggest that left ventricular diastolic stiffness was increased.

Heart rate increased significantly over time by 23% (from 63±14 to 78±14 beats/min, Figure 7 and Table 2-B). Stroke volume increased significantly by 20% (from 40±12 to 48±23 ml). Because of increased heart rate and stroke volume, cardiac output increased significantly by 52% (from 2500±1000 to 3800±2200 ml/min, Figure 8).

The pressure-volume loop measurements obtained at different afterloads were normal. A typical set of loops is shown in Figure 9.

Table 2-A: Aortic and Left Ventricular Pressures, and Ventriculoarterial Coupling Before Beta-blockade

	0 wk	1 wk	4 wk	8 wk	12 wk	Regression Equation [†]			s_d	s
AOP_{min} , mmHg	68	74	100	106	114	66	+	49 $(1 - e^{-t/4.1})$	6	8
	±12	±10	±13	±4	±6	±3		±4** ±1.1**		
AOP_{max} , mmHg	107	124	152	161	167	106	+	61 $(1 - e^{-t/3.0})$	11	10
	±7	±21	±11	±11	±6	±3		±4** ±0.7**		
P_{ED} , mmHg	7	10	14	14	14	7	+	7 $(1 - e^{-t/1.5})$	4	3
	±3	±4	±4	±4	±5	±1		±1** ±0.8		
P_{max} , mmHg	105	124	152	161	166	105	+	61 $(1 - e^{-t/2.9})$	10	10
	±7	±20	±12	±10	±7	±3		±3** ±0.6**		
P_{ES} , mmHg	102	119	149	159	163	§				
	±6	±20	±13	±10	±7					
E_a , mmHg/ml	2.9	3.3	3.0	4.2	4.0	3.0	+	0.1 t	1.3	0.7
	±1.3	±1.4	±0.8	±1.5	±1.5	±0.2		0.02**		
E_{max} / E_a	1.5	1.4	0.9	0.9	1.2	0.9	−	$0.05 (t - \bar{t}) + 0.01 (t - \bar{t})^2$	0.4	0.3
	±0.6	±0.4	±0.3	±0.5	±0.7	±0.1		0.01* 0.0*		

Data over time are mean ± standard deviation in 8 dogs. Parameter estimates are mean ± standard error. s_d = between-dogs variation. s = standard deviation of the mean squared residual error.

AOP_{min} = minimum diastolic aortic pressure; AOP_{max} = maximum systolic aortic pressure; P_{ED} = left ventricular end-diastolic pressure; P_{max} = maximum left ventricular pressure; P_{ES} = left ventricular end-systolic pressure; E_a = arterial elastance = P_{ES} / strokevolume; E_{max} = slope of the end-systolic pressure-volume relation; $\bar{t}$ = mean value of the time variable (approximately 5 weeks).

† Between-dog terms ($\Sigma b_i D_i$) omitted for clarity
§ Regression not determined.
* Regression coefficient is significantly different from zero; P≤0.05; ** P≤0.001.

Figure 5. In the unblocked state, aortic pressures increased exponentially during the 12 weeks after induction of renovascular hypertension . During acute beta-blockade induced by propranolol, the increases in aortic pressures were eliminated.

Figure 6. In the unblocked state, left ventricular end-diastolic pressure increased exponentially during the 12 weeks after induction of renovascular hypertension . During acute beta-blockade induced by propranolol, the increase in left ventricular end-diastolic pressure became linear.

Table 2-B: Hemodynamics and Left Ventricular Pump Function Before Beta-blockade

	0 wk	1 wk	4 wk	8 wk	12 wk	Regression Equation [†]	s_d	s
HR , beats/min	63 ±14	54 ±13	72 ±24	63 ±12	78 ±14	– ‡		
Stroke volume, ml	40 ±12	41 ±15	45 ±15	40 ±10	48 ±23	–		
Cardiac Output, ml/min	2500 ±1000	2300 ±1300	3100 ±1200	2500 ±500	3800 ±2200	–		
Stroke Work, mmHg ml	3900 ±1300	4600 ±2000	6100 ±2100	5900 ±1300	7200 ±3100	–		
dP/dt_{max} , mmHg/s	2800 ±400	3100 ±400	3500 ±500	3200 ±500	3400 ±500	–		
dP/dt_{min} , mmHg/s	-2500 ±200	-2800 ±300	-3200 ±400	-2800 ±400	-2900 ±300	–		
E_{max} , mmHg/ml	3.8 ±1.0	4.2 ±1.5	3.1 ±1.3	3.9 ±2.1	4.2 ±2.2	–		

Data over time are mean ± standard deviation in 8 dogs. Parameter estimates are mean ± standard error. s_d = between-dogs variation. s = standard deviation of the mean squared residual error.

HR = heart rate; dP/dt_{max} and dP/dt_{min} = maximum and minimum rates of pressure rise or fall; E_{max} = slope of the end-systolic pressure-volume relation;

† Between-dog terms ($\Sigma b_i D_i$) omitted for clarity
‡ Refer to pooled regression of unblocked and beta-blocked data shown in Table 3-B.
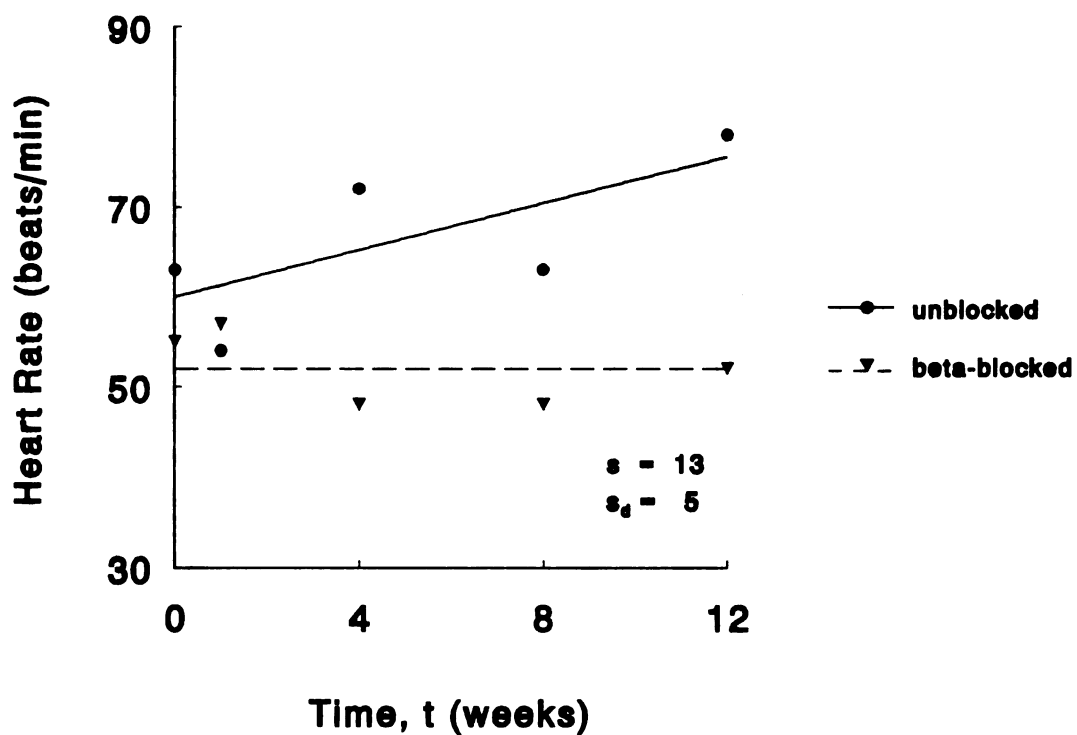
Figure 7. In the unblocked state, heart rate increased linearly during the 12 weeks after induction of renovascular hypertension. During acute beta-blockade induced by propranolol, the increases in heart rate were eliminated.
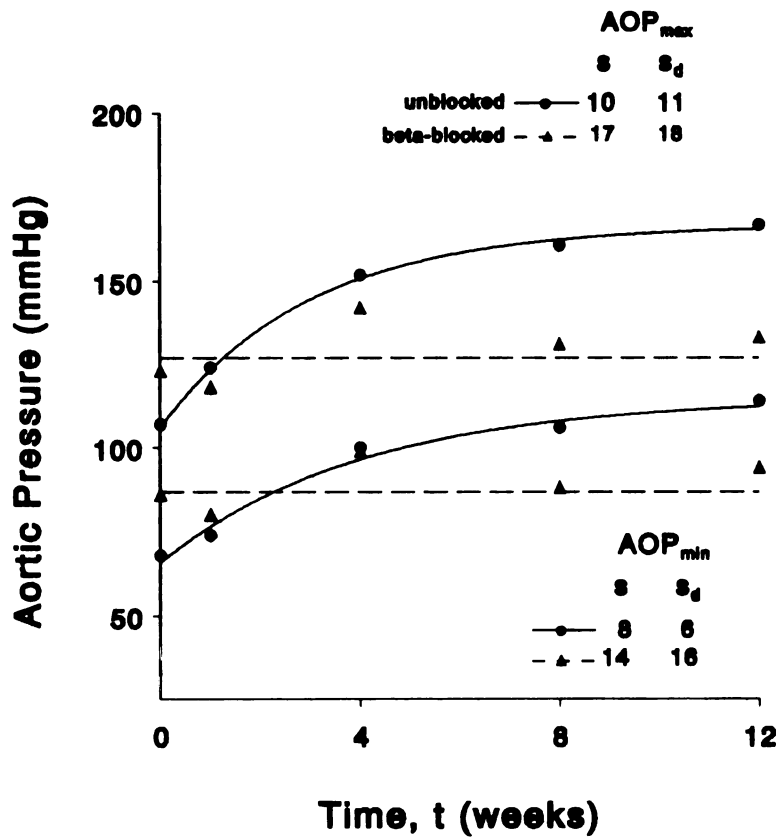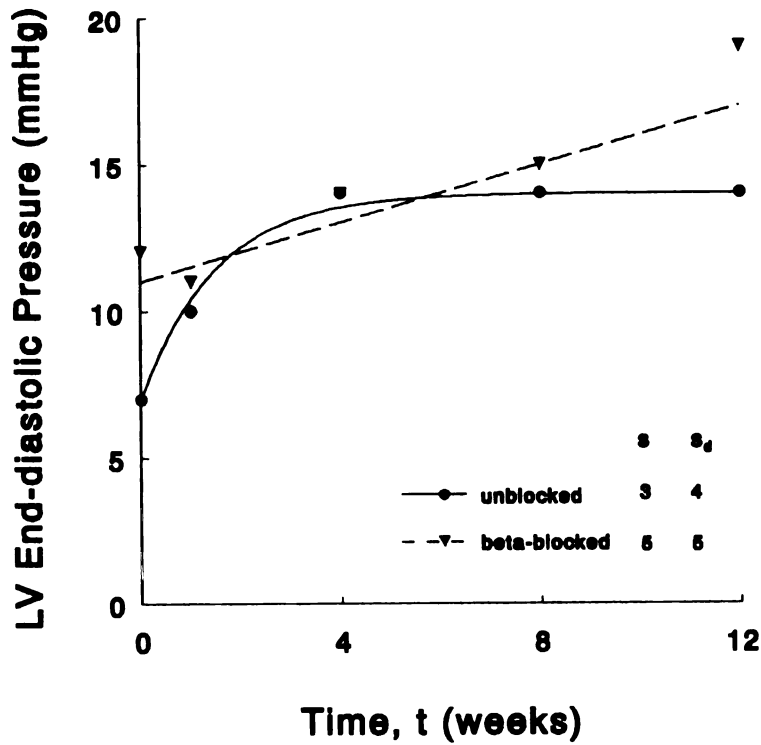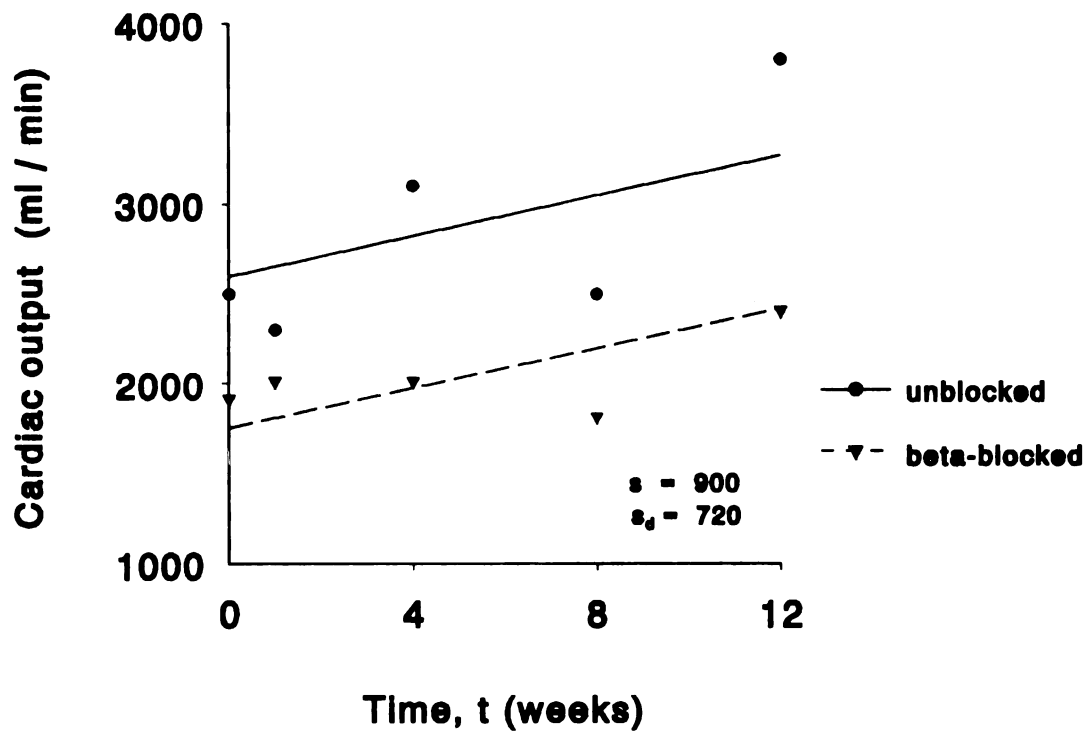
Figure 8. In the unblocked state, cardiac output increased linearly during the 12 weeks after induction of renovascular hypertension. During acute beta-blockade induced by propranolol, the cardiac output response was shifted downwards.

Figure 9. Left ventricular pressure-volume loops for 1 dog before and during acute beta-blockade. E$_{max}$, the slope of the end-systolic pressure-volume line, did not change significantly before acute beta-blockade, but it increased significantly over time during blockade. V$_d$, the volume axis intercept, did not change significantly over time before or during beta-blockade.

Indices of Contractility. Indices of contractility either increased significantly or remained unchanged over time in the unblocked state. This suggests that left ventricular contractility was not depressed during 12 weeks of pressure-overload hypertrophy. Stroke work and E_{max} increased linearly and significantly after renovascular hypertension. Stroke work increased 84% (from 3900±1300 to 7200±3100 mmHg ml, Figure 10). E_{max} increased 10% (from 3.8±1.0 to 4.2±2.2 mmHg/ml, Figure 11). dP/dt_{max} did not change significantly over time in the unblocked state (Table 2-B).

dP/dt_{min} also did not change significantly over time. However, dP/dt_{min} decreased in magnitude (by 19±8 mmHg/s per g) as the left ventricular wall mass increased in each dog. This result suggests that left ventricular relaxation was slowing down as the left ventricle hypertrophied.

Stroke work did not change significantly over the range of E_{max}/E_a values in the unblocked state.

$$SW = -4000 - 850 \; E_{max}/E_a + 100 \; V_{ED}$$
$$(\pm 2100) \quad (\pm 600) \quad\quad (\pm 20)$$
$$p=0.19 \quad\quad\quad p=0.0001$$

(Stroke work has units of mmHg ml, E_{max}/E_a is dimensionless, and V_{ED} has units of ml.) This finding indicates that the increased stroke work over time was not an effect of changes in ventriculoarterial coupling that occurred during hypertrophy.

Left Ventricular Function during Acute Beta-blockade

Hemodynamics. Acute beta-blockade with propranolol abolished the increases in aortic pressures and heart rate over time that were seen in the unblocked state.

Peak aortic and left ventricular systolic pressures did not change significantly from their initial means of 123±19 and 122±20 mmHg, respectively (Table 3-A,

Figure 5). Aortic diastolic pressure did not vary significantly from the initial mean of 86±17 mmHg. This response indicates that acute beta-blockade with propranolol successfully blocked the effects of beta-adrenergic stimulation throughout the 12-week study.

Left ventricular end-diastolic pressure increased 58% (from 12±9 to 19±6 mmHg, Table 3-A, Figure 6). This rise in diastolic pressure over time without changes in LV end-diastolic volume suggests that left ventricular diastolic stiffness was increased.

Heart rate was depressed by beta-blockade and did not change significantly over time from an initial mean of 55±13 beats/min, in contrast to the linear increase observed in the unblocked state. In other words, beta-blockade reduced the heart rate by a progressively larger amount over time (by -1.7±0.7 (SE) beats/min per week; Table 3-B, Figure 7), and brought the heart rate down to its initial level every time. These results suggest that the increase in heart rate over time was the result of increased beta-adrenergic stimulation.

In the acutely beta-blocked state, end-diastolic volume did not change significantly over time but end-systolic volume decreased slightly and significantly, indicating that systolic shortening was increased in the hypertrophied left ventricle (Table 3-B, Figure 4). End-diastolic volume did not vary from an initial mean of 98±7 ml. End-systolic volume decreased from 63±17 to 51±13 ml. Stroke volume increased from 35±12 to 46±10 ml per beat.

As a result of increased stroke volume, cardiac output also increased significantly over time (from 1900±700 to 2400±800 ml/min; Table 3-B, Figure 8).

As expected, V_d did not change significantly over time in the acutely beta-blocked state, consistent with the concept that V_d should be independent of inotropic state (50). V_d/V_w also did not change significantly over time.

Indices of Contractility. Acute beta-blockade reduced the magnitude of all indices of contractility relative to the unblocked state. However, all indices still increased significantly over time in the beta-blocked state, which suggests that in addition to increased beta-adrenergic stimulation, other factors are also contributing to improved left ventricular pump function, factors such as increased wall mass and intrinsic myocardial contractility.

Stroke work, dP/dt_{max}, and E_{max} all increased significantly and linearly over time during acute beta-blockade (Table 3-B). Stroke work increased 30% (from 3900 ± 1500 to 5100 ± 900 mmHg ml). dP/dt_{max} increased 14% (from 2100 ± 300 to 2400 ± 300 mmHg/s). E_{max} increased 62% (from 2.4 ± 0.5 to 3.9 ± 1.2 mmHg/ml).

Acute beta-blockade reduced the slope of the stroke work response by 60%, relative to the unblocked state (a decrease of -134 ± 50 from the unblocked slope of 210 ± 30 mmHg ml per week). This result shows that beta-adrenergic stimulation was a significant contributor to the stroke work increase over time. Stroke work decreased significantly as V_W increased (by -100 mmHg ml per g, Table 3-B), but only if the time variables were not included in the regression model, which suggests that this dependency on V_W is borderline significant. Stroke work increased significantly as E_{max}/E_a increased.

$$SW = -3200 + 960 \ E_{max}/E_a + 60 \ V_{ED}$$
$$(\pm 3000) \quad (\pm 300) \quad\quad\quad (\pm 30)$$
$$p\text{-}0.0024 \quad\quad\quad p\text{-}0.032$$

(Stroke work has units of mmHg ml, E_{max}/E_a is dimensionless, and V_{ED} has units of ml.) This result suggests that the improved left ventricular pump function observed during blockade results from the proportionally greater increase in E_{max} relative to arterial elastance.

dP/dt_{max} was significantly reduced by acute beta-blockade (by -1000±100 mmHg/s) compared to the unblocked state (Table 3-B). However, the magnitude of the reduction grew smaller over time (by 49±23 mmHg/s per week, Table 3-B). Thus, in effect, dP/dt_{max} actually increased over time by 49±23 mmHg/s per week in the beta-blocked state. dP/dt_{max} did not vary significantly as V_w increased.

Acute beta-blockade caused a downward parallel shift in E_{max} of -0.8±0.3 mmHg/ml from the unblocked state. There was no evidence that beta-blockade caused a slope change in E_{max} over time. In addition, increases in wall mass in each dog had no significant effect on E_{max}.

dP/dt_{min} did not change significantly over time, although it decreased significantly in magnitude (by 19±8 mmHg/s per g) as V_w increased. Acute beta-blockade caused a constant parallel shift in dP/dt_{min} (by 260±100 mmHg/s per g). These results indicate that left ventricular relaxation slowed down as the left ventricle hypertrophied, and that the slow down was not significantly dependent on changes in beta-adrenergic stimulation.

Table 3-A: Aortic and Left Ventricular Pressures, and Ventriculoarterial Coupling During Beta-blockade

	0 wk	1 wk	4 wk	8 wk	12 wk	Regression Equation [†]		s_d	s
AOP_{min} , mmHg	86	80	99	88	94	87	+ 0.6 t	16	14
	±17	±19	±25	±18	±19	±4	±0.5		
AOP_{max} , mmHg	123	118	142	131	133	127	+ 0.66 t	18	17
	±19	±12	±31	±19	±20	±5	±0.63		
P_{ED} , mmHg	12	11	14	15	19	11	+ 0.5 t	5	5
	±9	±6	±6	±6	±6	±1	±0.2*		
P_{max} , mmHg	122	113	137	125	133	124	+ 0.7 t	20	17
	±20	±15	±33	±22	±22	±5	±0.7		
P_{ES} , mmHg	120	112	132	120	131	§			
	±22	±15	±31	±21	±23				
E_a , mmHg/ml	3.9	3.5	3.2	3.4	3.1	3.7 −	0.05 t	1.2	0.7
	±1.8	±1.5	±1.3	±1.2	±1.0	±0.2	0.03 ns		
E_{max} / E_a	0.7	0.7	1.1	0.8	1.4	0.7	+ 0.05 t	0.3	0.5
	±0.3	±0.3	±0.6	±0.5	±0.6	±0.1	0.02**		

Data over time are mean ± standard deviation in 8 dogs. Parameter estimates are mean ± standard error. s_d = between-dogs variation. s = standard deviation of the mean squared residual error. All other variables are defined in Table 2-A.

† Between-dog terms ($\Sigma b_i D_i$) omitted for clarity.
§ Regression not determined.
* Regression coefficient is significantly different from zero, P≤0.05; ** P=0.02.
ns Not statistically significant.

Table 3-B: Hemodynamics and Left Ventricular Pump Function During Beta-blockade

	0 wk	1 wk	4 wk	8 wk	12 wk	Regression Equation †	Sd	s
HR, beats/min	55 ±13	57 ±7	48 ±9	48 ±9	52 ±15	$58 \pm 3 + 1.4t_{\pm 0.5^{**}} - 4.3B_{\pm 4.6\,ns} - 1.7Bt_{\pm 0.7^{**}}$	5	13
Stroke volume, ml	35 ±12	36 ±13	43 ±9	39 ±12	46 ±10	$40 \pm 2 + 0.5t_{\pm 0.2^{*}}$	11	8
Cardiac Output, ml/min	1900 ±700	2000 ±600	2000 ±200	1800 ±500	2400 ±800	$2600 \pm 200 + 56t_{\pm 24^{*}} - 850B_{\pm 200^{***}}$	720	900
Stroke Work ‡, mmHg ml	3900 ±1500	3600 ±900	5200 ±1200	4200 ±1400	5100 ±900	$-4000 \pm 900 + 210t_{\pm 30^{***}} - 1000B_{\pm 300^{**}} - 134Bt_{\pm 50^{**}} + 95V_{ED\,\pm 10^{***}}$	1400	900
						$-9000 \pm 1500 - 1700B_{\pm 200^{***}} - 100V_{W\,\pm 20^{***}} + 100V_{ED\,\pm 10^{***}}$	2000	1000
dP/dt$_{max}$, mmHg/s	2100 ±300	1900 ±300	2300 ±400	2300 ±500	2400 ±300	$1300 \pm 500 - 1000B_{\pm 130^{***}} + 40Bt_{\pm 20^{*}} + 10P_{ES\,\pm 3^{**}} - 1.7V_{ED\,\pm 4\,ns} - 6HR_{\pm 3^{*}}$	260	350
dP/dt$_{min}$, mmHg/s	-2500 ±200	-2500 ±300	-2500 ±800	-2400 ±400	-2300 ±300	$-2200 \pm 500 + 260B_{\pm 100^{*}} + 19V_{W\,\pm 8^{*}} - 8P_{ES\,\pm 2^{**}} - 6V_{ED\,\pm 4\,ns} - 3HR_{\pm 3\,ns}$	290	340
E$_{max}$, mmHg/ml	2.4 ±0.5	2.0 ±0.8	3.6 ±1.9	2.6 ±1.2	3.9 ±1.2	$3.3 \pm 0.3 + 0.08t_{\pm 0.04^{*}} - 0.8B_{\pm 0.3^{*}}$	0.8	1.4

Data over time are mean ± standard deviation in 8 dogs. Parameter estimates are mean ± standard error. B and V_W are defined in Table 1. Bt is the product of B and t. Bt represents a change in the effect of beta-blockade over time. All other variables are defined in Table 2-B.

† Between-dog terms ($\Sigma D_j D_j$) omitted for clarity.
§ Regression not determined.
‡ Two regressions are reported for stroke work, one vs. time and the other vs. wall mass.
* Regression coefficient is significantly different from zero; $P \leq 0.05$; ** $P \leq 0.001$; *** $P \leq 0.0001$.
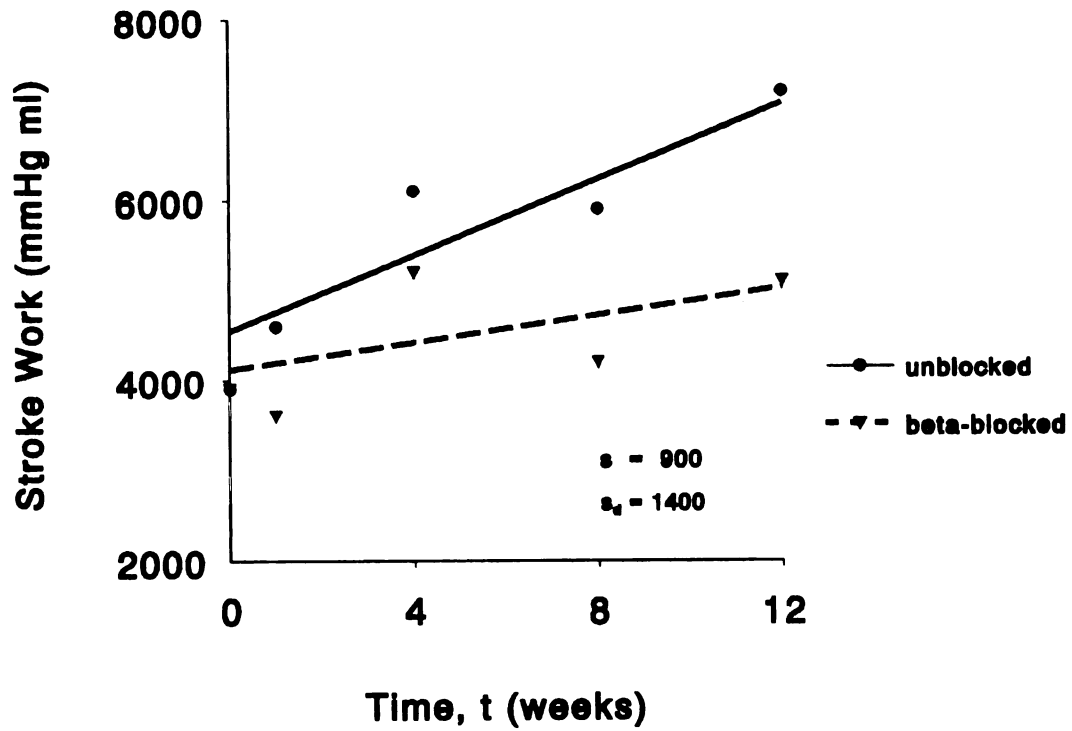ns Not statistically significant.

Figure 10. In the unblocked state, stroke work increased significantly during the 12 weeks after induction of renovascular hypertension. Acute beta-blockade reduced the magnitude of stroke work relative to the unblocked state, but this variable still increased significantly over time. Stroke work was also borderline dependent on wall mass.
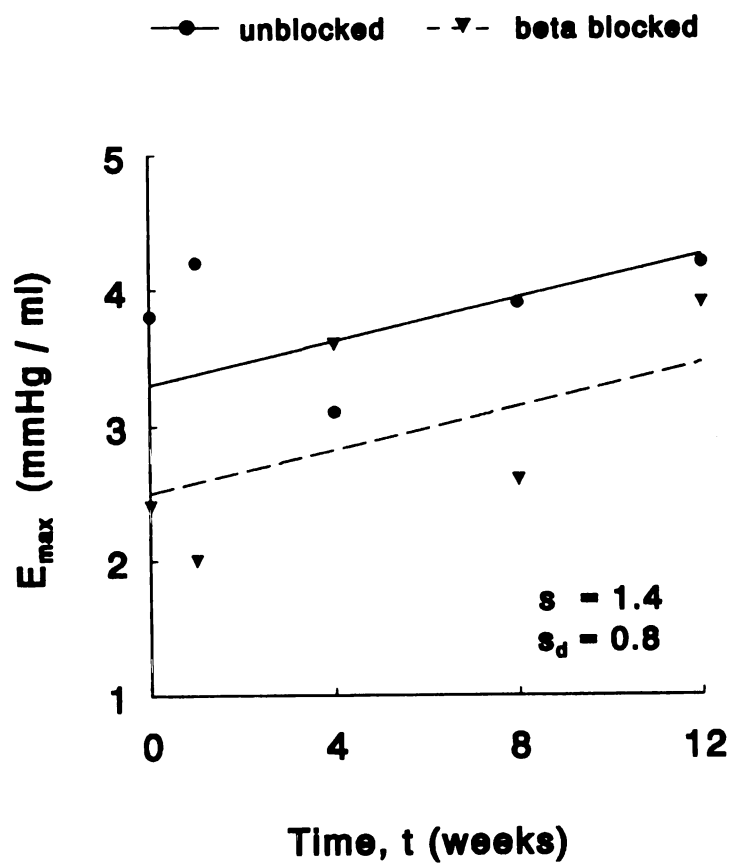
Figure 11. In the unblocked state, E_{max} increased significantly during the 12 weeks after induction of renovascular hypertension. Acute beta-blockade reduced the magnitude of E_{max} relative to the unblocked state, but E_{max} still increased significantly over time. E_{max} did not vary significantly with increases in LV wall mass.
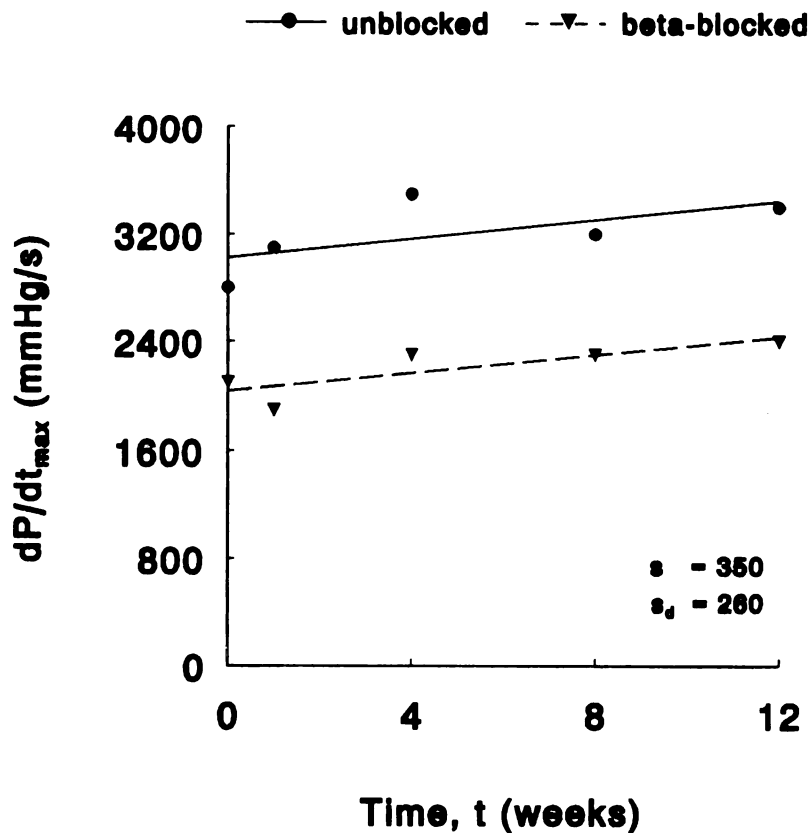
Figure 12. In the unblocked state, dP/dt_{max} did not change significantly during the 12 weeks after induction of renovascular hypertension. However, during acute beta-blockade, dP/dt_{max} increased significantly over time. Acute beta-blockade also reduced the magnitude of dP/dt_{max} relative to the unblocked state, dP/dt_{max} did not vary significantly with increases in LV wall mass. These patterns of changes in stroke work, E_{max}, and dP/dt_{max} suggest that beta-adrenergic stimulation is a major contributor to improved LV pump function and that the remaining improvements may be due to both increased intrinsic myocardial contractility and wall mass during pressure-overload hypertrophy induced by renovascular hypertension.
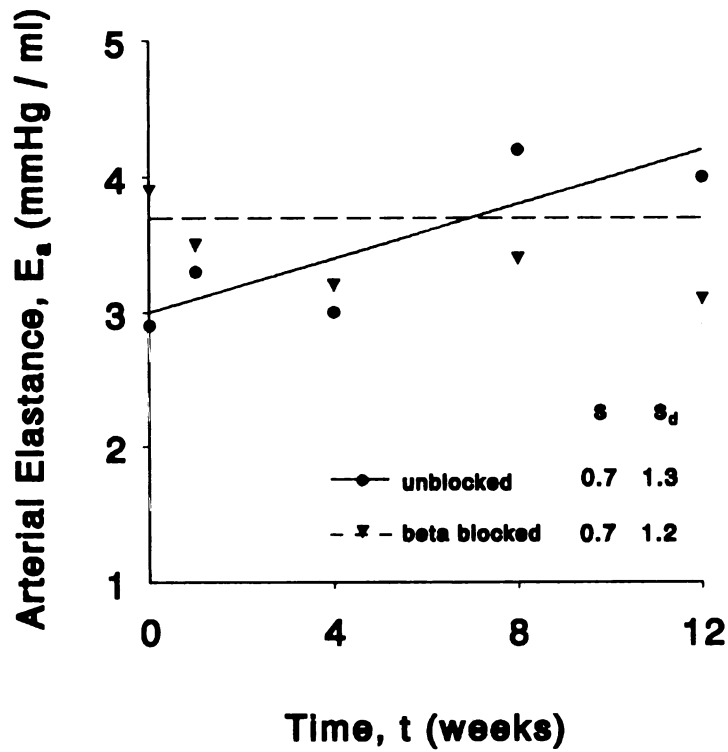
Figure 13. In the unblocked state, arterial elastance, E_a, increased linearly during the 12 weeks after induction of renovascular hypertension. During acute beta-blockade induced by propranolol, the increases in E_a were abolished.
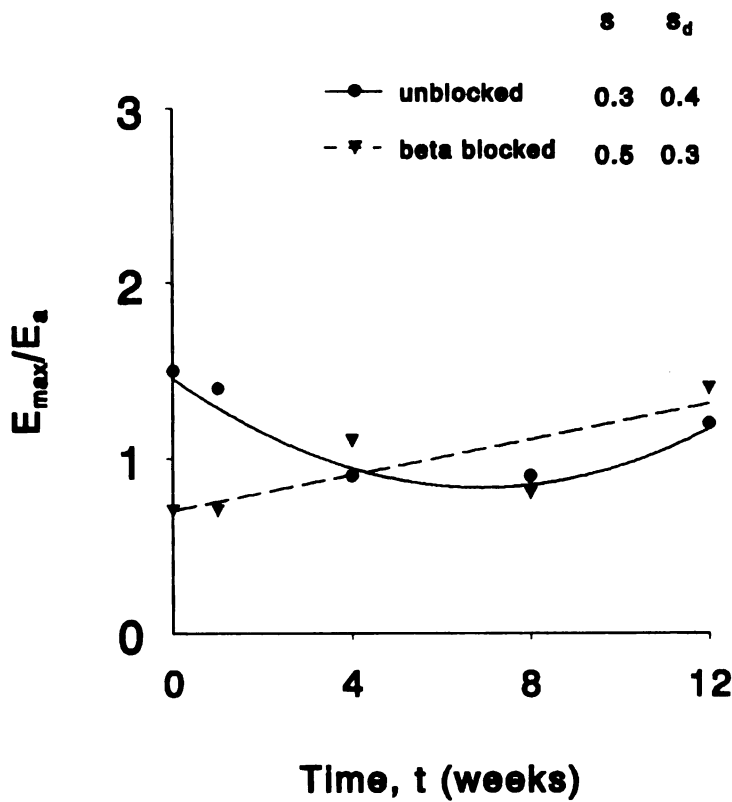
Figure 14. In the unblocked state, the ventriculoarterial coupling ratio of E_{max}/E_a decreased slightly in response to renovascular hypertension, then returned to near pre-hypertrophy levels 12 weeks after induction of renovascular hypertension. (These changes in ventriculoarterial coupling did not affect stroke work significantly in the unblocked state.) During acute beta-blockade induced by propranolol, E_{max}/E_a increased linearly over time.

DISCUSSION

This study of pressure-overload hypertrophy induced by renovascular hypertension in intact-chest dogs shows significantly improved left ventricular pump function over time, both before and during acute beta-blockade induced with propranolol, although beta-blockade did partially reduce indices of contractility relative to the unblocked state. The remaining improvement in pump function during beta-blockade was probably the effect of both increased wall mass and increased intrinsic contractility, although their exact contributions could not be determined.

Contribution of Increased Beta-adrenergic Stimulation

Beta-adrenergic stimulation appeared to have increased over time during pressure-overload hypertrophy, as evidenced by significantly increased heart rate, aortic pressures, and LV systolic pressures. These increases were unlikely to be the effects of decreased vagal stimulation; if they were vagally mediated, then acute beta-blockade by propranolol would not have abolished the increases. However, because propranolol did abolish these increases, they were probably the effect of increased beta-adrenergic stimulation, although other mechanisms which can be blocked by propranolol may also be involved.

The increased beta-adrenergic stimulation was a major contributor to improved left ventricular pump function as hypertrophy progressed, because when stimulation was blocked, indices of LV contractility decreased significantly. Stroke work, dP/dt_{max} , and E_{max} were smaller during blockade than in the unblocked state. In particular, stroke work at any given end-diastolic volume was reduced by 60% from the unblocked level.

Contribution of Increased Wall Mass and Intrinsic Contractility

Stroke work, dP/dt_{max}, E_{max}, and systolic shortening all increased over time in the beta-blocked state. If there were no changes in wall mass, then these increases would suggest that the intrinsic contractility of the myocardium had increased over time. However, because wall mass increased over time in pressure-overload hypertrophy, some investigators have attributed the increase in dP/dt_{max} to the presence of additional muscle fibers contracting in parallel, each of normal contractile function (7,37). In these studies, no measurements were made of changes in LV wall mass over time in each dog. Thus, the studies did not show conclusively that the increased dP/dt_{max} was associated with increased wall mass.

In the present study, V_W was measured repeatedly in each dog as hypertrophy progressed. Analysis by linear regression (described in Methods) showed that dP/dt_{max} and E_{max} did not vary significantly as V_W increased over time, and that stroke work may be borderline dependent on V_W (stroke work depended on V_W if the time variable was excluded from the regression, but was not dependent on V_W when time was included). Therefore, these results do not support the hypothesis that the improved LV function was due only to increased mass. Some factor other than increased mass also contributed to the increases in stroke work, dP/dt_{max}, E_{max}, and systolic shortening; this factor is probably increased intrinsic contractility.

Changes in LV Diastolic Stiffness and Relaxation

While LV systolic function appeared to improve over time, there was evidence that LV diastolic function was impaired. Left ventricular end-diastolic pressure, P_{ED}, increased rapidly over time in the unblocked state and reached a plateau at about 8 weeks. P_{ED} also increased over time in the beta-blocked state. These increases in P_{ED} occurred without significant changes in LV end-diastolic volume, which suggest that LV diastolic stiffness had increased, consistent with renovascular hypertension

(43,66).   In addition, dP/dt_{min} decreased significantly in magnitude as V_W increased. This change in dP/dt_{min} showed that diastolic relaxation was slowing down, but it is unclear whether this slow down is related to impaired LV function.

Angiotensin II may contribute to changes in LV diastolic function during renovascular hypertension. In a study of isolated, perfused rat hearts, Schunkert et al. found that angiotensin converting enzyme (ACE) activity and fractional conversion of angiotensin I to II were significantly increased in hypertrophied left ventricles (induced by aortic stenosis), but not in controls (55).   Infusion of angiotensin I caused a dose-dependent increase in LV end-diastolic pressure in hypertrophied left ventricles but not in controls; this difference was attributed to increased angiotensin II. Because the LV volume was held constant by a balloon, the increase in LV end-diastolic pressure signified a decrease in diastolic distensibility. Based on these findings, Schunkert et al. suggested that angiotensin II causes a dose-dependent depression of left ventricular diastolic relaxation in the hypertrophied rat left ventricle, possibly mediated by an increase in the "L-type" Ca^{++} current. Because plasma angiotensin II is elevated in renovascular hypertension, the increased LV end-diastolic pressure in the renovascular-hypertensive dogs could be an effect of increased angiotensin II.

Schunkert et al. reported that baseline dP/dt_{min} was more negative (larger magnitude) in hypertrophied ventricles than in controls, which is the opposite of our results from intact, anesthetized dogs. The reasons for this difference are unknown, but they may be an effect of the isolated heart procedure.

Changes in Ventriculoarterial Coupling

The increased stroke work before and during acute beta-blockade is not an effect of changes in ventriculoarterial coupling, E_{max}/E_a . Before blockade, stroke work did not vary significantly as E_{max}/E_a changed. During blockade, stroke work increased as E_{max}/E_a increased. However, the increase in E_{max}/E_a occurred because E_{max}

Increased while E_a remained constant. Thus, the increased stroke work was not a function of changing ventriculoarterial coupling or afterload mismatch.

Similarities and Differences between Pressure- and Volume-Overload Hypertrophy

Florenzano and Glantz's (15) study of volume-overload (eccentric) hypertrophy induced by aortic regurgitation is parallel in methods to this study of pressure-overload (concentric) hypertrophy induced by renovascular hypertension, so we can directly compare the effects of the two types of hypertrophy.

LV Pump Function. In volume-overload hypertrophy, LV pump function appeared to improve immediately in reaction to the creation of a lesion (puncture) in the aortic valve, but then remained unchanged over time following the lesion, whereas in pressure-overload hypertrophy, LV pump function continuously improved over time.

In volume overload, E_{max} increased as a result of the lesion but did not change further over time in the unblocked state, nor did E_{max} change in the acutely beta-blocked state. In pressure overload, E_{max} increased continuously during the 12-week study in both the unblocked and beta-blocked states. dP/dt_{max} did not change over time in either type of hypertrophy in the unblocked state, but it did increase over time during beta-blockade in pressure overload. Stroke volume did not change in volume overload, but it increased over time in pressure overload both before and after beta-blockade.

The pattern of change in E_{max} in volume overload was attributed to increased beta-adrenergic stimulation (15), whereas the changes in E_{max}, dP/dt_{max}, and stroke volume in pressure overload appear to depend not only on increased beta-adrenergic stimulation, but also on increased wall mass and intrinsic contractility.

Comparison of Hemodynamics. The volume changes observed in these studies of volume- and pressure-overload hypertrophy are consistent with eccentric and

concentric hypertrophy. As expected, volume-overload hypertrophy resulted in increased end-diastolic and end-systolic volumes and V_d over time. Pressure-overload hypertrophy did not change V_d or end-diastolic volumes, and decreased end-systolic volumes over time.

The pressure changes observed were also consistent with the stimulus of hypertrophy. Only diastolic pressures increased in volume-overload hypertrophy induced by aortic regurgitation. Both diastolic and systolic pressures increased in pressure-overload hypertrophy induced by renovascular hypertension.

During both volume- and pressure-overload hypertrophy, cardiac output decreased during acute beta-blockade. In addition, acute beta-blockade increased end-diastolic and end-systolic volumes (relative to the unblocked state) and reduced E_{max} , but beta-blockade did not change V_d . These effects are consistent with the negative inotropic effect of beta-blockade with propranolol.

Limitations of protocol

The indices of contractility that I used, dP/dt_{max} , E_{max} , and stroke work, all depend, to a greater or lesser degree, on preload (V_{ED}) and afterload (P_{ES}), which I accounted for using multiple linear regression. I also used linear regression to determine whether these indices covaried with LV wall mass. This regression approach to assess contractility is similar, in principle, to measuring changes in the slope of the dP/dt_{max}-end-diastolic volume or the stroke work-end-diastolic volume relationship (21,40). Although linear regression provided insights into how increased wall mass may influence LV pump function, it does not provide actual mechanisms.

Summary

The results of this study show significantly improved left ventricular pump function over time, both before and during acute beta-blockade induced with

propranolol, although beta-blockade did partially reduce indices of contractility relative to the unblocked state. This reduction indicates that increased beta-adrenergic stimulation was a major contributor to improved left ventricular pump function as hypertrophy progressed. The remaining improvement in pump function during beta-blockade could be the effect of changes in ventriculoarterial coupling, increased wall mass, or increased intrinsic contractility. The increased stroke work before and during acute beta-blockade was not an effect of changes in ventriculoarterial coupling, E_{max}/E_a. In addition, the results do not support the hypothesis that the remaining improved LV function was due only to increased mass. Some factor other than increased mass also contributed to the increases in stroke work, dP/dt_{max}, E_{max}, and systolic shortening. This factor is probably increased intrinsic contractility.

Chapter 5:   Left Ventricular Wall Stress

Introduction

The conventional wisdom about the effect of wall stress on ventricular hypertrophy is that there are two basic patterns (24). First, in volume-overload hypertrophy, end-diastolic (ED) wall stress increases and LV hypertrophy occurs until ED wall stress decreases back to normal levels, at which point hypertrophy stabilizes. Second, in pressure-overload hypertrophy, peak systolic wall stress increases and LV hypertrophy (specifically wall thickening) occurs until peak systolic wall stress decreases back to normal levels.

The hypothesis about pressure-overload hypertrophy is flawed because it does not account for patients who have hypertension (pressure-overload), significant hypertrophy (increased wall mass and thickness) and subnormal peak systolic wall stress. If hypertrophy occurs to "normalize" peak systolic wall stress, then these patients should not have subnormal wall stresses. In addition, there are hypertensive patients who do not have significant hypertrophy, but who have significantly lower systolic wall stresses than normal patients.   These variations in wall stress patterns suggest that the relationship between pressure overload, wall stress, and hypertrophy should be re-evaluated.

The patterns of systolic wall stress among patients with pressure-overload hypertrophy may depend on the type of hypertension. In a study of perinephritic hypertension in dogs, both end-diastolic and end-systolic wall stresses increase after induction of hypertension, but then decrease back to normal levels by 14 weeks (19,57). These results suggested that hypertrophy could normalize both end-diastolic and end-systolic wall stresses. In contrast, in a study of renovascular hypertension in

dogs, end-systolic wall tension did not increase significantly 3 weeks after renal artery constriction; end-diastolic wall tension was not reported (31). These results suggest that renal artery constriction may induce pressure-overload hypertrophy in the absence of elevated systolic wall stress, similar to "inappropriate hypertrophy". If systolic wall stress did not increase, could the hypertrophy have been induced by increased end-diastolic stress?

To determine whether increased end-diastolic rather than peak-systolic wall stress is associated with wall thickening in pressure-overload hypertrophy, the changes in both systolic and diastolic wall stress will be measured during the early development of hypertrophy (induced by renal hypertension).

Definitions of Mechanical Stress in the Left Ventricle

Wall Stress Estimation. Left ventricular mean circumferential wall stress was estimated using the thick-wall ellipsoid model of Falsetti et al. (14)

$$\sigma = \frac{Pa}{h} \frac{(2c^2 - a^2)}{(2c^2 + ah)}$$

P is internal pressure, h is the wall thickness, and a and c are the endocardial semi-minor and semi-major axes, respectively. Although this model is a simple one, it is adequate for purposes of describing global wall stress (45,70). The method of computing a and c from endocardial marker coordinates is described in Appendix A.

I used the echocardiographically-measured mean equatorial wall thickness to compute all circumferential wall stresses; this was considered to be fiber-corrected stress by Falsetti et al. (14), but not by Janz (32).

In the remainder of this dissertation, "wall stress" refers to circumferential wall stress.

<u>Fiber Stress Estimation.</u> I computed left ventricular mean fiber stress using the cylindrical model of Arts et al. (1).

$$\sigma_{fiber} = P_{LV}\left(1 + 3\frac{V_{LV}}{V_W}\right)$$

where P_{LV} is left ventricular (LV) pressure, V_{LV} is LV chamber volume, and V_W is the volume of the LV wall. The fiber stress data reported in this study were computed from the eigenvolume; this does not affect the qualitative changes in fiber stress over time.

RESULTS

Left Ventricular Wall Stress (unblocked state)

Left ventricular peak-systolic wall stress never increased as the left ventricle gradually hypertrophied. Instead it decreased linearly and significantly (from 220±50 to 140±20 mmHg, p=0.0001, Figure 15, Table 4). Similarly, mean-systolic, mean-ejection, and end-systolic wall stress all decreased linearly over time.

Left ventricular end-diastolic wall stress increased significantly after creation of hypertension but then decreased to pre-hypertrophy levels. End-diastolic stress increased from 19±11 mmHg at 0 weeks to 29±14 at 4 weeks, then decreased to 20±9 mmHg at 12 weeks, (p=0.03, Figure 16, Table 4).

Left Ventricular Fiber Stress (unblocked state)

Left ventricular (LV) end-systolic fiber stress increased exponentially (from 105±6 mmHg at week 0 to 165±7 mmHg at week 12); the time constant was 2.8±0.6 weeks which indicates that the increase should level off at about 14 weeks, consistent with the observed data.

Table 4:   Left Ventricular Wall Stress

	0 wk	1 wk	4 wk	8 wk	12 wk	Regression Equation [†]			s_d	s
$\sigma_{peak-systolic}$, mmHg	300 ±60	290 ±70	260 ±80	190 ±50	185 ±40	290 ±10	$-$	10 t ±1***	48	37
$\sigma_{mean-ejection}$, mmHg	250 ±50	250 ±50	230 ±70	170 ±50	160 ±40	250 ±8	$-$	8 t ±1***	44	30
$\sigma_{mean-systolic}$, mmHg	225 ±50	225 ±50	205 ±60	150 ±50	140 ±30	225 ±7	$-$	7 t ±1***	40	28
σ_{ES} , mmHg	150 ±50	150 ±30	145 ±50	110 ±40	115 ±40	150 ±7	$-$	3 t ±1**	34	28
σ_{ED} , mmHg	19 ±11	28 ±14	29 ±14	23 ±10	20 ±9	$29 - 1.7(t-\bar{t}) - 0.4(t-\bar{t})^2 + 0.1(t-\bar{t})^3$ ±2 ±1* ±0.1** ±0.03*			9	7
$\sigma_{fiber\ ES}$, mmHg	105 ±6	125 ±20	155 ±14	165 ±11	165 ±7	100 ±4	$+$	$65\,(1-e^{-t/2.8})$ ±4** ±0.6**	17	11
$\sigma_{fiber\ ED}$, mmHg	7 ±4	10 ±5	15 ±5	14 ±4	14 ±5	7 ±1	$+$	$8\,(1-e^{-t/1.4})$ ±1** ±0.8**	4	3

Data are mean ± standard deviation in 8 dogs.   Parameter estimates are mean ± standard error.

$\sigma_{peak-systolic}$ = peak-systolic wall stress; $\sigma_{mean-systolic}$ = mean-systolic wall stress; $\sigma_{mean-ejection}$ = mean-ejection wall stress; σ_{ES} = end-systolic wall stress;

σ_{ED} = end-diastolic wall stress; $\sigma_{fiber\ ES}$ = end-systolic fiber stress by Theo Arts's equation;

$\sigma_{fiber\ ED}$ = end-diastolic fiber stress; $\bar{t}$ = mean value of time variable (about 5 weeks).

† Between-dog terms ($\Sigma b_i D_i$) omitted for clarity.
* Regression coefficient is significantly different from zero, $P \leq 0.05$;   ** $P \leq 0.01$;   *** $P \leq 0.0001$.

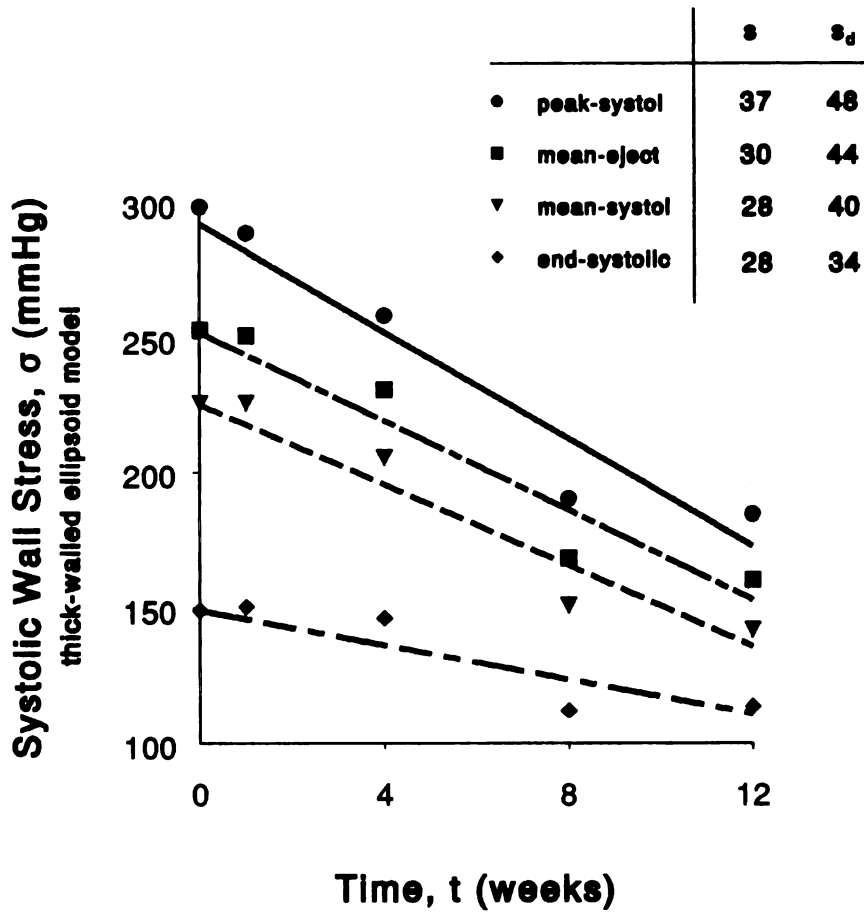|		s	s_d
●	peak-systol	37	48
■	mean-eject	30	44
▼	mean-systol	28	40
◆	end-systolic	28	34

Figure 15. Left ventricular systolic wall stress never increased, but instead decreased consistently and significantly over 12 weeks of renovascular hypertension. This decrease does not support the hypothesis that peak systolic wall stress increases during hypertension and that left ventricular wall thickening reduces systolic wall stress back to normal levels.
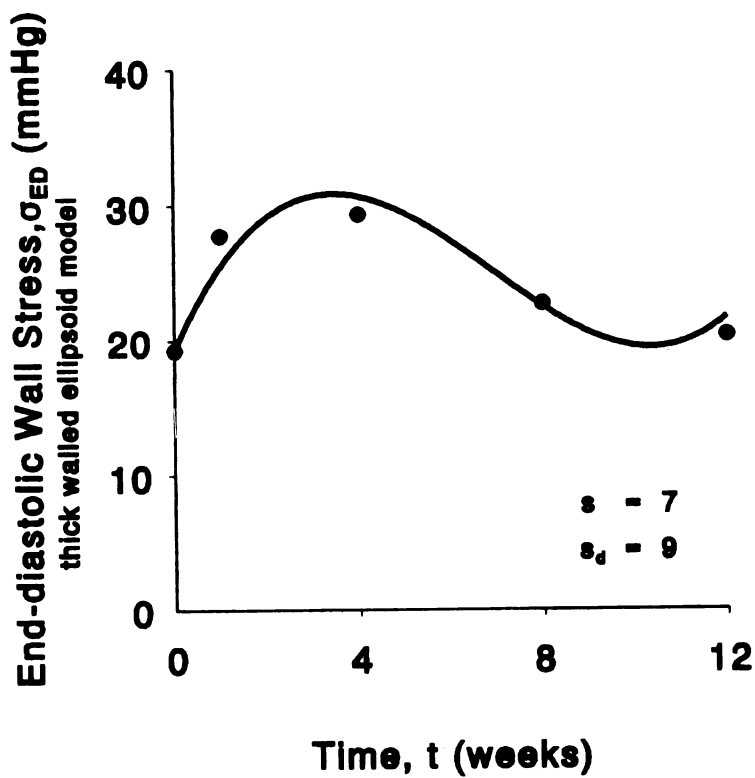
Figure 16. Left ventricular end-diastolic wall stress increased after induction of
renovascular hypertension, then decreased back to pre-hypertrophy values. This
pattern of changes suggest that the left ventricular wall thickens to maintain end-
diastolic wall stress at normal levels. (Because the linear, quadratic and cubic
coefficients were all significant, the response of the data was modeled as a third-order
polynomial in this figure.)

Figure 17. Left ventricular (LV) end-systolic fiber stress increased exponentially; the time constant was 2.8±0.6 weeks which indicates that the increase should level off at about 14 weeks, consistent with the observed data. Fiber stress was calculated using the equation $\sigma_{fiber} = P (1 + 3 V_{LV}/V_w)$ of Arts et al. (1), where P is LV pressure, V_{LV} is LV chamber volume, and V_w is the volume of the LV wall. The relationship between this model of fiber stress and wall thickening is unclear. After 12 weeks of renovascular hypertension, end-systolic fiber stress remains at a constant elevated level and shows no indication of returning to normal, despite significantly increased LV wall thickness.
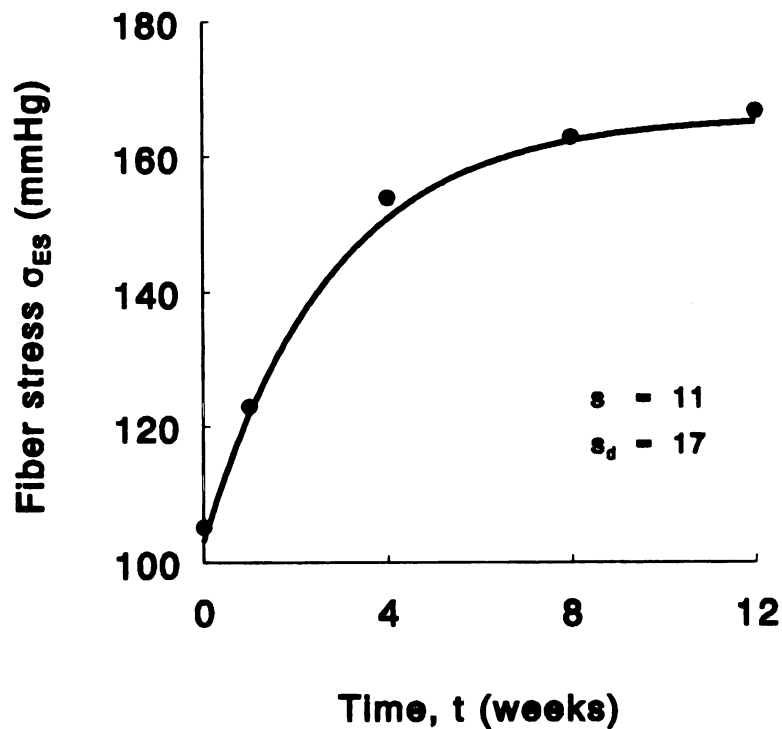
Figure 18. Left ventricular end-diastolic fiber stress increased exponentially; the time constant was 1.4±0.6 weeks which indicates that the increase reached a plateau at about 7 weeks. After 12 weeks of hypertension, end-diastolic fiber stress, like end-systolic fiber stress, remains at a constant elevated level and shows no indication of returning to normal, despite significantly increased LV wall thickness.
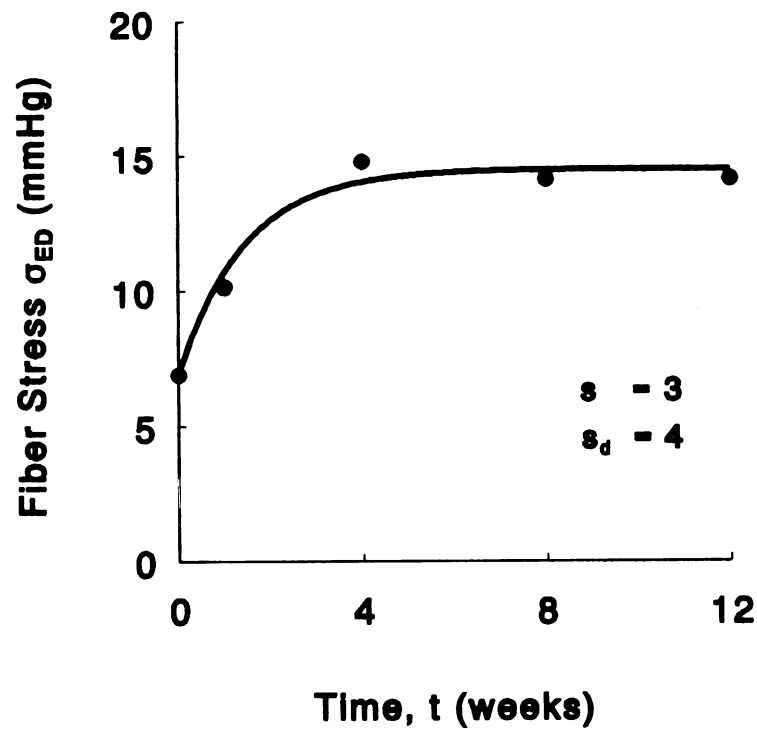
Similarly, LV end-diastolic fiber stress increased exponentially to twice the initial level (from 7±4 mmHg at week 0 to 14±5 mmHg at week 12); the time constant was 1.4±0.8 weeks which indicates that the increase should level off at about 7 weeks, or twice as fast as end-systolic fiber stress.

DISCUSSION

Similarities and Differences in Wall Stresses between Pressure- and Volume-Overload Hypertrophy

The end-diastolic wall stresses during volume-overload hypertrophy (induced by aortic regurgitation, Florenzano and Glantz (15)) and pressure-overload hypertrophy (induced by renovascular hypertension) both returned to control values as the heart hypertrophied, while the systolic stress patterns were different. In both forms of hypertrophy, the end-diastolic stress increased significantly after overload was induced, but then decreased significantly over time. End-diastolic stress returned to pre-hypertrophy values in renovascular hypertension and to near pre-hypertrophy values in volume overload as the heart hypertrophied. In volume overload, end-systolic stress did not change significantly over time, whereas in renovascular hypertension, all systolic stresses decreased significantly over time. These results in this model of renovascular hypertension suggest that the left ventricle hypertrophies to maintain normal end-diastolic stress, similar to volume-overload hypertrophy.

These findings bring an added complexity to our understanding of the stimuli to hypertrophy. The role of diastolic wall stress in pressure-overload hypertrophy has generally been de-emphasized because the conventional wisdom, as proposed by Grossman et al. (23,24), states that in pressure-overload hypertrophy the left ventricle hypertrophies in response to increased peak-systolic wall stress, and wall thickening

occurs to return peak-systolic stress to normal. Grossman et al. derived this hypothesis from a group of hypertensive human patients with pressure-overload (concentric) hypertrophy who had normal peak-systolic and end-diastolic wall stresses. Unfortunately, this hypothesis does not account for hypertensive patients without hypertrophy, nor does it account for patients who have hypertension and concentric hypertrophy but subnormal systolic wall stress, a condition which has been called "inappropriate hypertrophy" (63) because it does not conform to the Grossman hypothesis.

The predicted rise and fall of end-systolic wall stress during the development of pressure-overload hypertrophy has not been universally observed. During perinephritic hypertension in dogs, Shannon et al. observed that left ventricular end-systolic stress increased significantly 2-4 weeks after induction of hypertension, and that end-systolic stress returned to the same level as in sham-operated controls by 14 weeks (57). On the other hand, in a study of pressure-overload hypertrophy induced by aortic constriction in dogs, Sasayama et al. observed that the peak-systolic and end-systolic stresses in the same ventricles were significantly lower after 18 days of chronic pressure-overload hypertrophy than before hypertrophy, although peak-systolic (and end-diastolic) wall stress had increased after acute constriction, simultaneously with an increase in LV internal diameter (51). In contrast, during renovascular hypertension in dogs, Ison-Franklin et al. found no significant change in end-systolic wall tension after 3 weeks; they induced renovascular hypertension by constriction of both renal arteries (2-kidney, 2-clip) or by constriction of one renal artery and removal of the contralateral kidney (1-kidney, 1-clip) (31). In our study of renovascular hypertension in dogs (2-kidney, 1-clip), all systolic wall stresses decreased continuously over 12 weeks. These results call into question whether an increase in systolic stress is the mechanical stimulus to hypertrophy in all forms of hypertensive pressure-overload hypertrophy.

Interestingly, the end-diastolic wall stress changes are similar in aortic constriction and perinephritic and renovascular hypertension, even though their systolic wall stress patterns differ. Sasayama et al. showed that end-diastolic wall stress increased significantly after acute aortic constriction, but was not significantly different before and after an average of 18 days of chronic pressure-overload hypertrophy (51). Similarly, from the same group of dogs studied by Shannon et al. (57), Gelpi et al. reported that the end-diastolic wall stress increased significantly 2-4 weeks after induction of hypertension, then decreased back to control levels by 14 weeks (19). In our study, end-diastolic wall stress increased significantly after induction of hypertension, peaked at 4 weeks, then decreased to normal by 12 weeks. These results suggest the possibility that hypertrophy occurs to normalize end-diastolic wall stress in perinephritic and renovascular hypertension, and perhaps in hypertension induced by aortic constriction.

Our findings are consistent with results from humans studied by Shimizu et al. (58), who examined patients with a history of essential hypertension, arterial pressure exceeding 160/90 mmHg, and no evidence of coronary artery disease or symptoms of congestive heart failure. These patients were divided into two groups according to their left ventricular mass index (LVMI=LV mass/body surface area). One group had normal LVMI (within 2 standard deviations of the mean from normotensive controls), and the other had increased LVMI (greater than 2 standard deviations from the mean). The patients with increased LVMI had significantly lower peak-systolic, mean-systolic, and end-systolic wall stresses compared to normotensive controls. Furthermore, the hypertensive patients with normal LVMI also had lower peak-systolic wall stresses than normotensive controls. These systolic stress results are similar to those of our study; they do not support the hypothesis that pressure-overload hypertrophy occurs to normalize peak-systolic stress.

Our findings are also partially supported by results from human patients with "inappropriate hypertrophy". Sugishita et al. (63) studied hypertensive patients without hypertrophy, those with hypertrophy and normal end-systolic stress, and those with hypertrophy and subnormal end-systolic stress (inappropriate hypertrophy). None of these patients had hypertrophic cardiomyopathy or dilated cardiomyopathy. The patients were treated with a variety of antihypertensive drugs and reexamined in a follow up 4.4±1.7 (SD) years later. Because antihypertensive drugs reduce blood pressure and systolic wall stress, the Grossman hypothesis predicts that left ventricular mass should decrease. In fact, left ventricular mass did decrease in the patients without hypertrophy and in those who had hypertrophy with normal end-systolic stress. However, in patients with inappropriate hypertrophy, left ventricular mass actually increased significantly following antihypertensive therapy. Why? The increased hypertrophy could have been stimulated by increased diastolic wall stress, because several types of antihypertensive medications (beta-adrenergic blockers, arterial vasodilators, calcium antagonists, alpha-adrenergic blockers; reviewed in (16,39)) have been reported to increase diastolic wall stress. Unfortunately, Sugishita et al. did not report any diastolic wall stress data so I was not able to determine whether diastolic wall stress played a role in "inappropriate hypertrophy", which may actually be a very appropriate response to increased diastolic wall stress.

Increased diastolic wall stress results from stretch of the left ventricular wall during diastole. Sasayama et al. reported that the left ventricle adapts to hypertension induced by acute aortic constriction by initial dilation of the ventricular cavity, i.e. significantly increased end-diastolic diameter; end-diastolic wall stress increased simultaneously with the dilation (52). Stretch has been shown to trigger increased contractile protein synthesis in *in vitro* preparations of myocytes, papillary muscles, and isolated hearts. For example, when feline myocytes were deformed so that myocyte length increased by 10%, the result was an increase in the rate of incorporation of

[^{3}H]uridine into nuclear RNA and of [^{3}H]phenylalanine into cytoplasmic protein (47).

Sadoshima et al. showed that stretching rat myocytes causes rapid induction of c-fos

and other immediate-early genes followed by an increase in protein synthesis; they

suggested that the increase is modulated via stimulation of protein kinase C (49).

Kent et al. demonstrated that stretch of the ferret papillary muscle (either quiescent or

contracting) increases synthesis of both actin and myosin heavy chain, and that

myocardial protein synthesis was directly proportional to Na$^+$ influx; inhibiting sodium

influx decreased protein synthesis (34,35). These studies of myocytes and papillary

muscle all indicate that stretch leads to increased protein synthesis; they merely differ

on the exact signal pathway.

Stretch has also been shown to trigger increased contractile protein synthesis

in isolated hearts. Xenophontos et al. (69) showed that in the perfused rat heart,

increasing the aortic pressure from 60 mmHg to 120 mmHg (which stretches the left

ventricle) increased the rates of protein synthesis in both contracting and

tetrodotoxin-arrested hearts. These results show that passive stretch of the ventricle

does stimulate protein synthesis. Xenophontos et al. concluded that this increase

involved a cAMP-dependent mechanism that was independent of contractile activity.

In a similar study of isolated, perfused rat hearts, Schunkert et al. (56)

attempted to test the hypothesis that an acute increase in left ventricular systolic wall

stress, instead of passive diastolic wall stretch, was the stimulus for increased

induction of c-fos and c-jun mRNA (protooncogenes that may mediate protein

synthesis and cell growth in hypertrophy). A balloon was used inflate the left ventricle

to define set levels of volume (end-diastolic stress) and systolic wall stress in

contracting hearts and in relaxed hearts perfused with 2,3-butanedione monoxime

(BDM). Schunkert et al. found that in the contracting heart, c-fos mRNA levels were

proportional to the peak-systolic wall stress. Because this stress was also determined

by diastolic stretching of the left ventricle with the balloon, it was necessary to repeat

the measurements in relaxed hearts, which lack the contribution of active cross-bridge force generation. Schunkert et al. found that in the relaxed hearts, stretch did not have a significant effect on protooncogene induction. These results led Schunkert et al. to conclude that passive stretch (end-diastolic stress) is not the predominant signal for load-induced protooncogene induction. Unfortunately, this finding may be confounded by the use of BDM, which not only blocks cross-bridge cycling but has also been shown to block K$^+$, Na$^+$, and Ca^{++} channels (12,26,30,54), and to alter cAMP dependent protein kinase activity. Thus, it is possible that BDM blocked the mechanisms that transduce passive mechanical stretch into increased protein synthesis.

Factors other than stretch have also been shown to modulate hypertrophy, which may explain why the left ventricle changes shape differently in response to pressure overload than to volume overload. In pressure overload, the LV wall thickens while the lumen remains unchanged (concentric hypertrophy), whereas in volume overload, the LV wall remains at the same thickness while the lumen increases in size (eccentric hypertrophy). These differences may be the effects of norepinephrine, angiotensin II, and aldosterone (4,44,47,66,71).

Treatment with subpressor doses of norepinephrine cause hypertrophy of both the left and right ventricles (44). In this model of hypertrophy, the myocyte cross-sectional area increases significantly compared to control, and there is no change in the volume density of interstitial tissue. This pattern is similar to volume-overload hypertrophy, so norepinephrine probably does not cause the wall thickening associated with concentric hypertrophy.

The presence of angiotensin II and aldosterone have been shown to be necessary but not sufficient to cause hypertrophy (2,67,68). The combination of hypertension and the presence of elevated aldosterone causes growth in non-myocytes, specifically cardiac fibroblasts (66,68). Hypertension and elevated

levels of angiotensin II and aldosterone are characteristic of renovascular hypertension in which one or both renal arteries are constricted, thus reducing blood flow and pressure in the kidney. As a result, fibrosis occurs in interstitial and perivascular tissue, and the collagen volume fraction of the myocardium increases significantly. In hypertension models which do not involve renal artery constriction, such as perinephritic hypertension or infrarenal banding (aortic constriction distal to the renal arteries), there is no elevation of plasma angiotensin II and aldosterone, no fibrosis of the interstitial tissue, and no increase in collagen volume fraction (5,57). The difference between renovascular and non-renovascular hypertension may contribute to the structure of concentric hypertrophy. In perinephritic hypertension, wall thickness was increased 14 weeks after induction of hypertension, but the increase was not significantly different from sham-operated controls (57). In our study of renovascular hypertension, wall thickness increased significantly by 87% after 12 weeks compared to the initial values. The mechanisms that lead to these different patterns are unknown, but they may be modulated by angiotensin II and aldosterone.

Differences in the response of wall stress and wall thickening over time between this study and previous studies (9,17) may be related to the duration of the experiment. This study describes the early development of pressure-overload hypertrophy, during which end-diastolic stress increased then decreased back to normal, while systolic stress decreased continuously. In contrast, long-term (8-12 months) studies of chronic pressure-overload hypertrophy have shown that systolic and diastolic stresses were significantly increased at the end of the study (9,17). The contrasting responses is probably a function of the duration of pressure overload, because significant differences have been reported in the hypertrophic response of rat hearts at 8 weeks and 8 months after induction of renovascular hypertension by banding one renal artery (5,9). The left ventricle hypertrophies significantly after 8 weeks; the ratio of LV weight to body weight (LVW/BW) is 3.4 ± 0.2

(SEM) mg/g in banded rats versus 2.3±0.1 in controls (5). After 8 months, the LVW/BW ratio was 1.89±0.04 in banded rats versus 1.75±0.03 in controls (9), and the wall thickness was significantly lower in banded rats compared to controls. The changes in arterial pressure also varied over time--systolic pressure increased to 173±5 mmHg 2 weeks after banding and remained at this level for 5 months, then decreased to control levels by 8 months. These differences over time in the hypertrophic response may also occur in hypertensive dogs. In a 12-month study where pressure-overload hypertrophy was induced by aortic banding of 8-week old puppies, significant differences in muscle cross-sectional area between banded and control dogs were observed 3 months after banding; the differences grew progressively larger between 3 and 9 months, then did not change further afterwards (17). Furthermore, 6 of the 10 banded dogs developed left ventricular failure, characterized by significantly decreased midwall and endocardial shortening compared to control; these dogs also had significantly elevated systolic wall stresses at 12 months. I did not observe reduced shortening (decreased stroke volume) or increased systolic wall stresses in our 3-month study of developing renovascular hypertension in dogs, but these changes might have occurred if the duration of the study was longer.

Relation of Fiber Stress to Wall Thickening

The relationship between Art et al.'s fiber stress and wall thickening is unclear. After 12 weeks of renovascular hypertension, both end-systolic and end-diastolic fiber stress remain at a constant elevated level and show no indication of returning to normal, despite significantly increased LV wall thickness.

The Arts et al. model of fiber stress is a simple one and may not represent true fiber stress at all points throughout the myocardium. Janz (32) contends that to compute fiber stress at a point in the myocardium, one must know the dominant fiber angle and both the circumferential and meridional stresses. Thus, fiber stress remains

a less useful measure of mechanical stress in the heart than circumferential wall stress, because fiber stress is more difficult to estimate.

Summary

This study of pressure-overload hypertrophy induced by renovascular hypertension in intact-chest dogs shows that, in contrast to accepted theory, left ventricular systolic circumferential wall stresses decreased significantly over time. In contrast, end-diastolic circumferential wall stress increased following renal artery constriction, then returned to baseline values as the heart hypertrophied. This pattern of wall stress changes resembles that of volume-overload hypertrophy, in which end-diastolic stress increased significantly after volume overload was induced, then decreased significantly over time to near pre-hypertrophy values, while end-systolic stress remained unchanged over time. These results suggest that both volume- and pressure-overload hypertrophy normalizes end-diastolic, not peak systolic or end-systolic wall stress.

Chapter 6:   Left Ventricular Contraction Patterns

Introduction

By tracking the positions and movements of implanted endocardial markers with biplane cineradiography, it is possible to determine how the left ventricular cavity changes its shape and contraction pattern over time as it hypertrophies. Using linear transformation methods from continuum mechanics, Walley et al. quantified the magnitudes and directions of deformation of the left ventricle (65) from the coordinates of the markers. Their analysis revealed that the contraction of the normal left ventricle is a nearly homogeneous deformation, consisting of dilations or contractions along three mutually perpendicular principal directions, e.g. base-apex, anterior-posterior, and septum-free wall (25,65). Whether the contraction pattern of the left ventricle changes during pressure or volume overload was, however, unknown.

In this study, the deformation analysis of Walley et al. is performed on normal, pressure-overload, and volume-overload hearts to determine whether the left ventricle continues to deform homogeneously after hypertrophy, whether it deforms in the same principal directions, how much it deforms in each direction, and whether the type of hypertrophy affects the direction and magnitudes of deformation.

Deformation Pattern

Starting with the coordinates of markers at end-diastole and end-systole, I computed the linear transformation, T, that maps end-diastolic coordinates onto their end-systolic coordinates, following Walley et al. (65).

The three dimensional coordinates of n markers is recorded as a 3 x n matrix X.

$$X = \begin{bmatrix} x_1 & x_2 & \cdots & x_n \\ y_1 & y_2 & \cdots & y_n \\ z_1 & z_2 & \cdots & z_n \end{bmatrix}$$

If we assume that the ventricle deforms homogeneously, then the position of the markers at time t, X(t), relative to a reference position, in this case X_{ED}, is described by a linear transformation T(t). $X(t) = T(t)\ X_{ED}$ where T(t) is a 3 x 3 matrix. Given the coordinates at two different times, we can estimate T(t) as

$$\hat{T}(t) = X(t)(X_{ED})^T \left[X_{ED}\ (X_{ED})^T \right]^{-1}$$

T can be decomposed uniquely into two component transformations, a rotation, R, and a dilatation, D, where T = R D. The rotation transformation R quantifies the solid-body rotation of the left ventricle, independent of contraction. The dilatation transformation D quantifies the change in size and shape of the left ventricle.

T, R and D were computed for each frame of film in each dog.

Accuracy of T transformation

The issue of how accurately T describes the deformation of the left ventricle has been addressed by Walley et al. (65), who showed that T can predict the end-systolic location of markers within 2mm of their actual positions (Table 2 and Figure 5 of Walley et al. (65)). They achieved better agreement than 2mm in most of the hearts. This small variation is due to the fact that the left ventricle does not precisely follow the mathematical assumption of homogeneous deformation used to derive T. The variation is much less than the actual displacement of the endocardial wall between end-diastole and end-systole (Table 2 of Walley et al. (65)).

To evaluate the accuracy of the predicted coordinates, Walley et al. defined a measure of fit analogous to a standard correlation coefficient,

$$ r = \sqrt{1 - \frac{SS_{res}}{SS_{tot}}} $$

where SS_{res} is the sum of squared distances (three-dimensional) between the actual and predicted marker positions, and SS_{tot} is the sum of squared distances between actual marker positions at end-diastole and end-systole.

In closed-chest, normal dogs, the transformations from end-diastolic to end-systolic coordinates yielded r values from 0.838 to 0.996; the median was 0.968 (65). The high correlations show that the differences between the predicted and actual coordinates were small compared to the distance that the markers move between end-diastole and end-systole. In other words, the errors produced by assuming homogeneous deformation are small relative to the total deformation.

In this dissertation, I extended the validation of the linear transformations to hearts that have pressure- or volume-overload hypertrophy. The following types of transformations were estimated:

1) ED_0-ED_{12} denotes the transformation from the end-diastolic (ED) coordinates at week 0 to the ED coordinates at week 12. This transformation describes the changes in the LV end-diastolic shape that occur as a result of hypertrophy.

2) ED_{12}-ES_{12} denotes the transformation from the ED coordinates at week 12 to the end-systolic (ES) coordinates at week 12. This transformation describes the contraction pattern of the hypertrophied left ventricle during systole.

The r values obtained from these transformations are comparable to those reported by Walley et al. The transformation from ED_0 to ED_{12} yielded a median r of 0.963 for pressure overload and 0.975 for volume overload (Table 5). The transformation from ED_{12} to ES_{12} yield medians of r=0.955 and r=0.961 for pressure and volume overload,

respectively. These results indicate that in hypertrophied hearts, the assumption of homogeneous deformation still produces relatively small errors compared to the total deformation.

The high accuracy of the ED_0 to ED_{12} transformation suggests that the LV cavity changes its shape homogeneously during both pressure and overload hypertrophy. In addition, the high accuracy of the ED_{12} to ES_{12} transformation indicates that the hypertrophied left ventricle contracts nearly homogeneously in both forms of hypertrophy, similar to before hypertrophy.

Orientation of Principal Directions of Deformation

The principal directions of contraction or dilation are defined by the three orthogonal eigenvectors of the dilatation transformation D. This transformation is estimated as

$$D - (f^T f)^{1/2}$$

Each eigenvector is associated with a scalar eigenvalue that is equal to the fractional change in length along the direction of the eigenvector as the heart and the implanted markers deform from one configuration to another.

Do the principal directions of deformation and the eigenvalues change during hypertrophy? To answer this question, I reduced the eigenvectors to three orientation angles--Euler "space-three" angles (defined in Figure 19 and Appendix B)--and analyzed the changes in the angles and eigenvalues using linear regression.

Linear Regression Model

The Euler Angles and eigenvalues were modeled by the following regression equation:

$$y - b_0 + b_H H + b_{HK} HK + b_C C + \sum b_i D_i$$

where H, HK, C, and D_i are dummy variables; H represents the presence or absence of hypertrophy; HK is the effect of pressure- versus volume-overload hypertrophy; C is the variation between end-diastole and end-systole. The D_i variables were defined in Chapter 2 (effects coding).

$$H = \begin{cases} 0 \text{ before hypertrophy (week 0)} \\ 1 \text{ after hypertrophy (week 12)} \end{cases}$$

$$HK = \begin{cases} 0 \text{ before hypertrophy (week 0)} \\ 1 \text{ pressure-overload hypertrophy (week 12)} \\ -1 \text{ volume-overload hypertrophy (week 12)} \end{cases}$$

$$C = \begin{cases} -1 \text{ at end-diastole} \\ 1 \text{ at end-systole} \end{cases}$$

If b_H is significantly different from zero, then the presence of hypertrophy causes an increase or decrease in y. If b_{HK} is significant, then pressure- and volume-overload hypertrophy have opposite effects on y. If b_C is significant, then y changes significantly between end-diastole and end-systole.

Effect of Hypertrophy on Euler Angles and Eigenvalues

Hypertrophy did not have a significant effect on any of the three Euler angles (Table 6). Left ventricular contraction from end-diastole to end-systole increased angles α_1 and α_3, by approximately 22 and 42 degrees, respectively, which indicates that the orientations of the principal directions of deformation changed during systole

(Table 6). A positive α_1 rotation is a counterclockwise rotation around the x axis (looking from the right to the left side), and a positive α_3 rotation is a counterclockwise rotation around the z axis (looking from the tail to the head). The combination of positive α_1 and α_3 rotations indicate that the base (valve ring) of the left ventricular long axis rotates down and towards the left side during systole. Because hypertrophy did not have a significant effect on the Euler angles, these results indicate that the orientations of the principal directions of deformation were the same before and after hypertrophy.

Pressure- and volume-overload hypertrophy did not change eigenvalue λ_1 significantly, which indicated that the LV cavity did not change its length along the long axis. Hypertrophy did not change λ_3, but did cause a small significant change in eigenvalue λ_2; λ_2 is larger in volume overload by approximately 0.12 relative to pressure overload (Table 7). Because the eigenvectors associated with eigenvalues λ_2 and λ_3 are radial vectors (in the short-axis plane), the change in λ_2 suggests that the cross-section of the left ventricular cavity became more elliptical during pressure-overload hypertrophy (Table 7).

As expected, all eigenvalues decreased significantly between end-diastole and end-systole, consistent with contraction of the ventricular cavity during systole (Table 7).

Summary

In hypertrophied hearts, the assumption of homogeneous deformation produces relatively small errors compared to the total deformation. The change in the end-diastolic shape of the left ventricular cavity during hypertrophy was also nearly homogeneous in both forms of hypertrophy. Hypertrophy did not have a significant effect on any of the three Euler angles, which indicates that the principal directions of deformation are the same before and after hypertrophy. Hypertrophy did have a slight

effect on the amount of dilatation in one principal direction, in the cross-sectional (short axis) plane of the left ventricle. Analysis of the stretches (eigenvalues) in the principal directions indicated that one radial stretch was significantly smaller in pressure-overload than in volume overload (by 12%), and indicates that the cross-section of the pressure overloaded left ventricle is more elliptical than that of the volume overloaded ventricle. There was no change in principal stretch in the direction of the long axis.

Table 5: Correlations Between Predicted and Observed Three-Dimensional Marker Positions

Experiment	ED0 to ED12	ED12 to ES12
Pressure Overload		
704	0.992	0.954
707	0.942	0.956
708	0.996	0.917
709	0.925	0.914
710	0.984	0.966
712	0.844	0.955
713	0.895	0.972
714	0.986	0.906
Group Median:	0.963	0.955
Volume Overload		
511	0.962	0.978
513	0.974	0.954
514	0.995	0.967
516	0.976	0.946
Group Median:	0.975	0.961
Median of Pooled Data:	0.975	0.955

ED0 to ED12 denotes the transformation from the end-diastolic (ED) coordinates at week 0 to the ED coordinates at week 12. This transformation describes the changes in the LV end-diastolic shape that occur as a result of hypertrophy.

ED12 to ES12 denotes the transformation from the ED coordinates to the end-systolic (ES) coordinates at week 12. This transformation describes the contraction pattern of the hypertrophied left ventricle during systole.
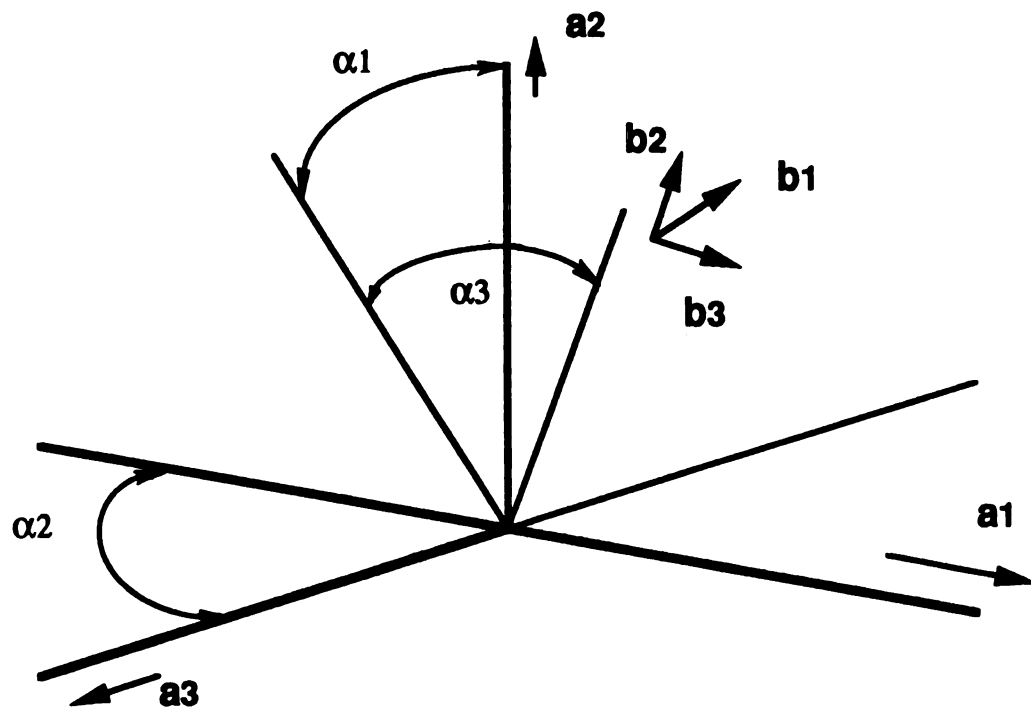
Figure 19. Definition of Euler "space-three" orientation angles. The vectors a_1, a_2, a_3, and b_1, b_2, b_3 are two sets of orthogonal, right-handed unit vectors. The angles α_1, α_2, α_3 represent the rotations that describe the orientation of the vectors b_i relative to a_i, where $i = 1,2,3$. To obtain orientations b_i from a_i, first superimpose b_i on a_i, then perform an a_1 rotation of α_1 degrees (i.e. a counterclockwise rotation of α_1 degrees in the a_2-a_3 plane), then an a_2 rotation of α_2, and finally an a_3 rotation of α_3. In this study, a_1 is the left-right axis ($+a_1$ = right), a_2 is the ventral-dorsal axis ($+a_2$ = dorsal), and a_3 is the cranial-caudal axis ($+a_3$ = caudal). The conversions from vectors to Euler angles are described in Appendix B.

Table 6:   Euler *Space-three* Angles

Angle	Point during Cardiac Cycle	Pooled Baseline Data at 0 Weeks	After 12 Weeks of Pressure Overload	After 12 Weeks of Volume Overload
α_1, degrees	ED	31 ± 47	70 ± 40	18 ± 70
	ES	55 ± 48	84 ± 54	49 ± 85
α_2	ED	-27 ± 26	-17 ± 33	7 ± 38
	ES	−26 ± 51	-20 ± 35	-12 ± 35
α_3	ED	48 ± 94	80 ± 71	53 ± 52
	ES	103 ± 93	128 ± 74	48 ± 47

Angle	Regression Equation [†]						
α_1	43 ± 7	+	20 H ± 10 ns	−	3 HK ± 10 ns	+	11 C ± 5 *
α_2	-26 ± 6	+	16 H ± 9 ns	−	12 HK ± 9 ns	−	2 C ± 4 ns
α_3	75 ± 14	+	13 H ± 22 ns	−	8 HK ± 22 ns	+	21 C ± 10 *

Data are mean ± standard deviation for 8 dogs with pressure-overload hypertrophy and 4 dogs with volume-overload hypertrophy. Parameter estimates are mean ± standard error.

H, HK, and C are dummy variables. H is presence or absence of hypertrophy; H = 0 before hypertrophy (week 0) and H = 1 at 12 weeks. HK is the effect of pressure versus volume overload hypertrophy; HK = 0 before hypertrophy, HK = 1 after 12 weeks of pressure overload, and HK = −1 after 12 weeks of volume overload. C is variation at two points in the cardiac cycle; C = −1 at end-diastole and C = 1 at end-systole.

† Between-dog terms ($\Sigma b_i D_i$) omitted for clarity.
* Regression coefficient is significantly different from zero; $P \leq 0.05$.
ns Not statistically significant.

Table 7:   Eigenvalues

Eigenvalue	Point during Cardiac Cycle	Pooled Baseline Data at 0 Weeks	After 12 Weeks of Pressure Overload	After 12 Weeks of Volume Overload
λ_1 (= λ_{LONG})	ED	1.01 ± 0.02	1.07 ± 0.17	1.04 ± 0.10
	ES	0.96 ± 0.06	0.97 ± 0.11	0.92 ± 0.10
λ_2	ED	1.00 ± 0.01	0.96 ± 0.09	1.02 ± 0.13
	ES	0.77 ± 0.11	0.77 ± 0.11	0.83 ± 0.14
λ_3	ED	0.99 ± 0.02	1.02 ± 0.11	1.00 ± 0.15
	ES	0.78 ± 0.10	0.79 ± 0.17	0.71 ± 0.20

Eigenvalue	Regression Equation [†]
λ_1	0.98 ± 0.02 + 0.02 H ± 0.02 ns + 0.02 HK ± 0.02 ns − 0.04 C ± 0.01 **
λ_2	0.89 ± 0.02 + 0.02 H ± 0.03 ns − 0.06 HK ± 0.03 * − 0.10 C ± 0.01 ***
λ_3	0.89 ± 0.02 − 0.01 H ± 0.03 ns + 0.03 HK ± 0.03 ns − 0.12 C ± 0.01 ***

Data are mean±standard deviation for 8 dogs with pressure-overload hypertrophy and 4 dogs with volume-overload hypertrophy. Parameter estimates are mean±standard error.

λ_{LONG} is the eigenvalue associated with the long axis of the left ventricle. λ_2 and λ_3 are associated with two radial eigenvectors that, together with the long axis, completes a right-handed orthogonal basis. These radial vectors vary in orientation between hearts.

The dummy variables H, HK, and C are defined in Table 6.

† Between-dog terms ($\Sigma b_i D_i$) omitted for clarity.
* Regression coefficient is significantly different from zero, $P \leq 0.05$; ** $P \leq 0.01$; *** $P \leq 0.001$.
ns Not statistically significant.

Chapter 7:   Conclusions

Left Ventricular Wall Stress

This study of pressure-overload hypertrophy induced by renovascular hypertension in intact-chest dogs shows that, in contrast to accepted theory, left ventricular systolic circumferential wall stresses decreased significantly over time. In contrast, end-diastolic circumferential wall stress increased following renal artery constriction, then returned to baseline values as the heart hypertrophied. This pattern of wall stress changes resembles that of volume-overload hypertrophy, in which end-diastolic stress increased significantly after volume overload was induced, then decreased significantly over time to near pre-hypertrophy values, while end-systolic stress remained unchanged over time. These results suggest that both volume- and pressure-overload hypertrophy normalizes end-diastolic, not peak systolic or end-systolic wall stress.

LV Pump Function

The results of this study show significantly improved left ventricular pump function over time, both before and during acute beta-blockade induced with propranolol, although beta-blockade did partially reduce indices of contractility relative to the unblocked state. This reduction indicates that increased beta-adrenergic stimulation was a major contributor to improved left ventricular pump function as hypertrophy progressed. The remaining improvement in pump function during beta-blockade could be the effect of changes in ventriculoarterial coupling, increased wall mass, or increased intrinsic contractility. The increased stroke work before and during acute beta-blockade was not an effect of changes in ventriculoarterial coupling, E_{max}/E_a.

In addition, the results do not support the hypothesis that the remaining improved LV function was due only to increased mass. Some factor other than increased mass also contributed to the increases in stroke work, dP/dt_{max}, E_{max}, and systolic shortening. This factor is probably increased intrinsic contractility.

LV Contraction Patterns

In hypertrophied hearts, the assumption of homogeneous deformation still produces relatively small errors compared to the total deformation. The change in the end-diastolic shape of the left ventricular cavity during hypertrophy was also nearly homogeneous in both forms of hypertrophy. Hypertrophy did not have a significant effect on any of the three Euler angles, which indicates that the principal directions of deformation are the same before and after hypertrophy. Hypertrophy did have a slight effect on the amount of dilatation in one principal direction, in the cross-sectional (short axis) plane of the left ventricle. Analysis of the stretches (eigenvalues) in the principal directions indicated that one radial stretch was significantly smaller in pressure-overload than in volume overload, and indicates that the cross-section of the pressure overloaded left ventricle is more elliptical than that of the volume overloaded ventricle. There was no change in principal stretch in the direction of the long axis.

Implications to Diagnosis of "Inappropriate Hypertrophy"

In this study, the conclusion that hypertrophy occurs to normalize left ventricular end-diastolic wall stress in both volume and pressure overload resolves a long standing paradox known as "inappropriate hypertrophy", a condition in which patients have hypertension (pressure overload) and concentric hypertrophy, but subnormal systolic wall stress. The paradox exists because the conventional hypothesis about pressure-overload hypertrophy is that increased peak-systolic circumferential wall stress stimulates LV hypertrophy and that LV wall thickening decreases peak-systolic

wall stress. The conventional hypothesis is wrong. If this hypothesis were correct, then ventricles with <u>subnormal</u> systolic wall stress should not be hypertrophied--yet this condition exists. This form of hypertrophy was dubbed "inappropriate hypertrophy" because it did not fit the conventional hypothesis.

In contrast, our results indicate that the mechanical stimulus to left ventricular hypertrophy is increased end-diastolic stress in both pressure and volume overload, so "inappropriate hypertrophy" ceases to be a paradox; this condition is a perfectly appropriate response to increased end-diastolic stress. Indirect evidence from the studies of Sugishita et al. (63) supports this new hypothesis. In their study, patients with "inappropriate hypertrophy" were treated with a variety of antihypertensive drugs and reexamined in a follow up 4.4±1.7 (SD) years later. They found that although the antihypertensive drugs reduced blood pressure (decreased pressure overload), these patients actually had <u>increased</u> hypertrophy. This increase is probably the effect of increased diastolic wall stress, because several types of antihypertensive drugs are known to increase diastolic wall stress (39). Thus, the results of Sugishita et al. are consistent with our results, and suggest that the appropriate treatment for patients with "inappropriate hypertrophy" is to reduce end-diastolic wall stress.

REFERENCES

1. Arts T., P.H.M. Bovendeerd, F.W. Prinzen, and R.S. Reneman. Relation between left ventricular cavity pressure and volume and systolic fiber stress and strain in the wall. Biophys. J. 59:93-102, 1991.

2. Baker K.M., M.I. Chernin, S.K. Wixson, and J.F. Aceto. Renin-angiotensin system involvement in pressure-overload cardiac hypertrophy in rats. Am. J. Physiol. 259:H324-H332, 1990.

3. Belcher P., L.E. Boerboom, G.N. Olinger. Standardization of end-systolic pressure-volume relation in the dog. Am. J. Physiol. 249:H547-553, 1985.

4. Ben L.K., J. Maselli, L.C. Keil, and I.A. Reid. Role of the renin-angiotensin system in the control of vasopressin and ACTH secretion during the development of renal hypertension in dogs. Hypertension 6:35-41, 1984.

5. Brilla C.G., R. Pick, L.B. Tan, J.S. Janicki, K.T. Weber. Remodeling of the Rat Right and Left Ventricles in Experimental Hypertension. Circ. Res. 67:1355-1364, 1990.

6. Brooks, D.P., and T.A. Fredrickson. Use of Ameroid Constrictors in the Development of Renin-Dependent Hypertension in Dogs. Lab. Anim. Sci. 42:67-69, 1992.

7. Broughton A., and P.I. Korner. Left ventricular pump function in renal hypertensive dogs with cardiac hypertrophy. Am. J. Physiol. 251:H1260-H1266, 1986.

8. Bustamante J.O., A. Ruknudin, and F. Sachs. Stretch-activated channels in heart cells: Relevance to Cardiac Hypertrophy. J. Cardiovasc. Pharmacol. 17 (Suppl. 2): S110-S113, 1991.

9. Capasso J.M., T. Palackal, G. Olivetti, and P. Anversa. Left Ventricular Failure Induced by Long-term Hypertension in Rats. Circ. Res. 66:1400-1412, 1990.

10. Carlsson E., and E.N.C. Milne. Permanent implantation of endocardial tantalum screws: A new technique for functional studies of the heart in the experimental animal. J. Can. Assoc. Radiol. 18:304-309, 1967.

11. Chagas A.C.P., and S.A. Glantz. Angiographic validation of eigenvolume to measure left ventricular size. Circ. Res. 62:1237-1246, 1988.

12. Coulombe A., I.A. Lefevre, E. Deroubaix, D. Thuringer, and E. Coraboeuf. Effect of 2,3-Butanedione 2-Monoxime on Slow Inward and Transient Outward Current in Rat Ventricular Myocytes. J. Mol. Cell. Cardiol. 22:921-932, 1990.

13. Davis P.L., G.L. Raff, and S.A. Glantz. A method to identify implanted radiopaque markers despite rotation of the heart. Am. J. Physiol. 239:H573-H580, 1980.

14. Falsetti H.L., R.E. Mates, C. Grant, D.G. Greene, and I.G. Bunnell. Left ventricular wall stress calculated from one-plane cineangiography: An approach to force-velocity analysis in man. Circ. Res. 26:71-84, 1970.

15. Florenzano F., and S.A. Glantz. Left ventricular mechanical adaptation to chronic aortic regurgitation in intact dogs. Am. J. Physiol. 252:H969-H984, 1987.

16. Frohlich E.D. Regression of Cardiac Hypertrophy and Left Ventricular Pumping Ability Postregression. J. Cardiovasc. Pharmacol. 17(Suppl. 2):S81-S86, 1991.

17. Gaasch W.H., M.R. Zile, P.K. Hoshino, C.S. Apstein, A.S. Blaustein. Stress-Shortening Relations and Myocardial Blood Flow in Compensated and Failing Canine Hearts with Pressure-Overload Hypertrophy. Circulation 79:872-883, 1989.

18. Gelpi R.J., L. Hittinger, A.M. Fujii, V.M. Crocker, I. Mirsky, and S.F. Vatner. Sympathetic Augmentation of Cardiac Function in Developing Hypertension in Conscious Dogs. Am. J. Physiol. 255:H1525-H1534, 1988.

19. Gelpi R.J., A. Pasipoularides, A.S. Lader, T.A. Patrick, N. Chase, L. Hittinger, R.P. Shannon, S.P. Bishop, and S.F. Vatner. Changes in Diastolic Cardiac Function in Developing and Stable Perinephritic Hypertension in Conscious Dogs. Circ. Res. 68:555-567, 1991.

20. Glantz S.A., and B.K. Slinker. Primer of Applied Regression and Analysis of Variance. New York, McGraw-Hill, Health Professions Division, 1990.

21. Glower D.D., J.A. Spratt, N.D. Snow, J.S. Kabas, J.W. Davis, C.O. Olsen, G.S. Tyson, D.C. Sabiston, and J.S. Rankin. Linearity of the Frank-Starling relationship in the intact heart: the concept of preload recruitable stroke work. Circulation 71:994-1009, 1985.

22. Grant C., D.G. Greene, and I.L. Bunnell. Left ventricular enlargement and hypertrophy: A clinical and angiographic study. Am. J. Med. 39:895-904, 1965.

23. Grossman W. Cardiac Hypertrophy: Useful Adaptation or Pathologic Process? Am. J. Med. 69: 576-84, 1980.

24. Grossman W., D. Jones, and L.P. McLaurin. Wall stress and patterns of hypertrophy in the human left ventricle. J. Clin. Invest. 56:56-64, 1975.

25. Grover M., and S.A. Glantz. Endocardial pacing site affects left ventricular end-diastolic volume and performance in the intact anesthetized dog. Circ. Res. 53:72-85, 1983.

26. Gwathmey J.K., R.J. Hajjar, and R.J. Solaro. Contractile Deactivation and Uncoupling of Crossbridges: Effects of 2,3-Butanedione Monoxime on Mammalian Myocardium. Circ. Res. 69:1280-1292, 1991.

27. Hannaford B., and S.A. Glantz. Adaptive linear predictor tracks implanted radiopaque markers. IEEE Trans. Biomed. Eng. 32:117-125, 1985.

28. Hayashida K., K. Sunagawa, M. Noma, M. Sugimachi, H. Ando, and M. Nakamura. Mechanical Matching of the Left Ventricle with the Arterial System in Exercising Dogs. Cir. Res. 71:481-489, 1992.

29. Horowitz S., and S.A. Glantz. Analog to digital data conversion and display system. San Francisco, University of California at San Francisco Cardiology Computer Facility, 1979.

30. Huang G., and J.J. McArdle. Novel Suppression of an L-type Calcium Channel In Neurones of Murine Dorsal Root Ganglia by 2,3-butanedione monoxime. J. Physiol. 447:257-274, 1992.

31. Ison-Franklin E.L., B.R. Coleman, and L.N. Cothran. Absence of Increase In Left Ventricular Mass In Dogs with Bilateral Renovascular Hypertension. Am. J. Hypertens. 1:131S-136S, 1988.

32. Janz R.F. Estimation of local myocardial stress. Am. J. Physiol. 242:H875-H881, 1982.

33. Kane T.R., P.W. Likins, and D.A. Levinson. Spacecraft Dynamics. pp30-38. McGraw-Hill Book Co., New York, 1983.

34. Kent R.L., J.K. Hoober, and G. Cooper IV. Load Responsiveness of Protein Synthesis in Adult Mammalian Myocardium: Role of Cardiac Deformation Linked to Sodium Influx. Circ. Res. 64:74-85, 1989.

35. Kent R.L., D.L. Mann, and G. Cooper IV. Signals for Cardiac Muscle Hypertrophy In Hypertension. J. Cardiovasc. Pharmacol. 17 (Suppl. 2): S7-S13, 1991.

36. Kono A., W.L. Maughan, K. Sunagawa, K. Hamilton, K. Sagawa, M.L. Weisfeldt. The use of left ventricular end-ejection pressure and peak pressure in the estimation of the end-systolic pressure-volume relationship. Circulation 70(6): 1057-1065, 1984.

37. Korner P.I., A. Bobik, G.L. Jennings, J.A. Angus, and W.P. Anderson. Significance of Cardiovascular Hypertrophy in the Development and Maintenance of Hypertension. J. Cardiovasc. Pharmacol. 17(Suppl. 2): S25-S32, 1991

38. Krahwinkel O.J., D.C. Sawyer, G.E. Egster, and G. Bender. Cardiopulmonary effects of fentanyl-droperidol, nitrous oxide and atropine sulfate in dogs. Am. J. Vet. Res. 36:1211-1219, 1975.

39. Leenen F.H.H., and E. Harmsen. Antihypertensive Drugs and Cardiac Trophic Mechanisms. J. Cardiovasc. Pharmacol. 17(Suppl. 2):S50-57, 1991.

40. Little W.C. The Left Ventricular dP/dt_{max}-End-Diastolic Volume Relation in Closed-Chest Dogs. Circ. Res. 56:808-815, 1985.

41. Little W.C., and C.P. Cheng. Left Ventricular-Arterial Coupling in Conscious Dogs. Am. J. Physiol. 261(1 Pt 2):H70-76, 1991.

42. Long C.S., K. Kariya, L. Karns, and P.C. Simpson. Sympathetic Activity: Modulator of Myocardial Hypertrophy. J. Cardiovasc. Pharmacol. 17(Suppl. 2):S20-S24, 1991.

43. Lorell B., and W. Grossman. Cardiac Hypertrophy: The Consequences for Diastole. J. Am. Coll. Cardiol. 9(5):1189-1193, 1987.

44. Marino T.A., M. Cassidy, D.R. Marino, N.L. Carson, and S. Houser. Norepinephrine-Induced Cardiac Hypertrophy of the Cat Heart. Anat. Rec. 229:505-510, 1991.

45. McHale P.A., and J. Greenfield. Evaluation of several geometric models for estimation of left ventricular circumferential wall stress. <u>Circ. Res.</u> 33:303-312, 1973.

46. Misbach G.A., and S.A. Glantz. Changes in the diastolic pressure-diameter relation alter ventricular function curves. <u>Am. J. Physiol.</u> 237:H644-H648, 1979.

47. Morgan H.E., and K.M. Baker. Cardiac hypertrophy: Mechanical, neural, and endocrine dependence. <u>Circulation</u> 83:13-25, 1991.

48. Raff G.L., and S.A. Glantz. Volume loading slows left ventricular isovolumic relaxation rate: Evidence of load-dependent relaxation in the intact dog heart. <u>Circ. Res.</u> 48:813-824, 1981.

49. Sadoshima J., and S. Izumo. Signal Transduction Pathways of Stretch-Induced Hypertrophy in Neonatal Rat Cardiac Myocytes <u>In Vitro.</u> <u>Circulation</u> 86(Suppl. I):I95, 1992.

50. Sagawa K., H. Suga, A.A. Shoukas, K.M. Bakalar. End-systolic pressure/volume ratio: a new index of ventricular contractility. <u>Am. J. Cardiol.</u> 232:748-753, 1977.

51. Sasayama S., D. Franklin, and J. Ross Jr. Hyperfunction with normal inotropic state of the hypertrophied left ventricle. <u>Am. J. Physiol.</u> 232:H418-H425, 1977.

52. Sasayama S., J. Ross Jr., D. Franklin, C.M. Bloor, S. Bishop, and R.B. Dilley. Adaptations of the left ventricle to chronic pressure overload. <u>Circ. Res.</u> 38:172-178, 1976.

53. Schiller N.B., C.G. Skioldebrand, E.J. Schiller, C.C. Mavroudis, N.H. Silverman, S.H. Rahimtoola, and M.J. Lipton. Canine left ventricular mass estimation by two-dimensional echocardiography. Circulation 68:210-216, 1983.

54. Schlichter L.C., P.A. Pahapill, and I. Chung. Dual Action of 2,3-Butanedione Monoxime (BDM) on K^+ Current in Human T Lymphocytes. J. Pharmacol. Exp. Ther. 261(2):438-446, 1992.

55. Schunkert H., V.J. Dzau, S.S. Tang, A.T. Hirsch, C.S. Apstein, and B.H. Lorell. Increased Rat Cardiac Angiotensin Converting Enzyme Activity and mRNA Expression in Pressure Overload Left Ventricular Hypertrophy: Effects on Coronary Resistance, Contractility, and Relaxation. J. Clin. Invest. 86:1913-1920, 1990.

56. Schunkert H., L. Jahn, S. Izumo, C.S. Apstein, B.H. Lorell. Localization and regulation of c-fos and c-jun protooncogene induction by systolic wall stress in normal and hypertrophied rat hearts. Proc. Natl. Acad. Sci. 88:11480-11484, 1991.

57. Shannon, R.P., R.J. Gelpi, L. Hittinger, D.E. Vatner, C.J. Homey, R.M. Graham, and S.F. Vatner. Inotropic Response to Norepinephrine is Augmented Early and Maintained Late in Conscious Dogs with Perinephritic Hypertension. Circ. Res. 68:543-554, 1991.

58. Shimizu G., Y. Hirota, Y. Kita, K. Kawamura, T. Saito, and W.H. Gaasch. Left Ventricular Midwall Mechanics in Systemic Arterial Hypertension: Myocardial

Function Is Depressed in Pressure-Overload Hypertrophy. Circulation 83:1676-1684, 1991.

59. Slinker B.K., A.C.P. Chagas, and S.A. Glantz. Chronic pressure overload hypertrophy decreases direct ventricular interaction. Am. J. Physiol. 253:H347-H357, 1987.

60. Spann J.F. Jr., R.A. Buccino, E.H. Sonnenblick, and E. Braunwald. Contractile state of cardiac muscle obtained from cats with experimentally produced ventricular hypertrophy and heart failure. Circ. Res. 21:341-354, 1967.

61. Suga H., R. Hisano, Y. Goto, and O. Hamada. Normalization of end-systolic pressure-volume relation and E_{max} of different sized hearts. Jpn. Circ. J. 48:136-143, 1984.

62. Suga H., O. Yamada, Y. Goto, Y. Igarashi, Y. Yasumura, and T. Nozawa. Reconsideration of normalization of E_{max} for heart size. Heart and Vessels 2:67-73, 1986.

63. Sugishita Y., K. Iida, and K. Yukisada. Mechanical and Non-mechanical Factors in Hypertensive Hypertrophy, Their Clinical Roles. Jpn. Circ. J. 54:568-574, 1990.

64. Van de Velde E.T., D. Burkhoff, P. Steendijk, J. Karsdon, K. Sagawa, and J. Baan. Nonlinearity and load sensitivity of end-systolic pressure-volume relation of canine left ventricle in vivo. Circulation 83:315-327, 1991.

65. Walley K.R., M. Grover, G.L. Raff, J.W. Benge, B. Hannaford, and S.A. Glantz. Left ventricular dynamic geometry in the intact and open chest dog. Circ. Res. 50:573-589, 1982.

66. Weber K.T. and C.G. Brilla. Pathological Hypertrophy and Cardiac Interstitium. Fibrosis and Renin-Angiotensin-Aldosterone System. Circulation 83:1849-1865, 1991.

67. Weber K.T., C.G. Brilla, J.S. Janicki. Signals for the Remodeling of the Cardiac Interstitium in Systemic Hypertension. J. Cardiovasc. Pharmacol. 17 (Suppl. 2): S14-S19, 1991.

68. Weber K.T., C.G. Brilla, J.S. Janicki, H.K. Reddy, and S.E. Campbell. Myocardial fibrosis: role of ventricular systolic pressure, arterial hypertension, and circulating hormones. Bas. Res. Cardiol. 86 (Suppl 3): 25-31, 1991.

69. Xenophontos X.P., P.A. Watson, B.H. Chua, T. Haneda, and H.E. Morgan. Increased cyclic AMP content accelerates protein synthesis in rat heart. Circ. Res. 65(3):647-656, 1989.

70. Yin F.C.P. Ventricular wall stress. Circ. Res. 49:829-842, 1981.

71. Young D.B. Comparison of a beta-blocker and converting enzyme inhibitor in two types of experimental hypertension, in Laragh J.H., Buhler F.R. and Seldin D.W. (eds): Frontiers in Hypertension Research. New York, Springer-Verlag New York Inc., p. 436-439, 1981.

APPENDIX A

Fitting an ellipsoid to endocardial marker coordinates.

Each left ventricle contains between 8 and 13 implanted endocardial markers, each with its own (x y z) coordinates. I used these coordinates to find a best-fit ellipsoid for the endocardial surface.

First, I translated the marker coordinates to the origin (0 0 0) of the fixed-axis coordinate system. The apical marker was defined as the new origin by subtracting its coordinate from all marker coordinates.

$$
\begin{bmatrix} x'_i \\ y'_i \\ z'_i \end{bmatrix} = \begin{bmatrix} x_i \\ y_i \\ z_i \end{bmatrix} - \begin{bmatrix} x_{apex} \\ y_{apex} \\ z_{apex} \end{bmatrix}
$$

where $(x_i \ y_i \ z_i)$ is the coordinate of marker i.

Next, I defined the long axis of the left ventricle as the vector n that connects the apical marker at $(x_{apex} \ y_{apex} \ z_{apex})$ to the aortic valve midpoint at $(x_{valve} \ y_{valve} \ z_{valve})$. The magnitude of n is

$$
\mid n \mid = \sqrt{(x_{valve} - x_{apex})^2 + (y_{valve} - y_{apex})^2 + (z_{valve} - z_{apex})^2}
$$

The markers were then rotated twice to make the long axis parallel to the z axis. First, the markers were rotated counterclockwise by an angle Θ in the x-y plane to bring the long axis into the x=0 plane (the y-z plane), then they were rotated clockwise by an angle ϕ in the y-z plane to superimpose the long axis on the z axis.

The rotation matrix for angle Θ was defined as

$$R_\Theta - \begin{bmatrix} \cos\Theta & -\sin\Theta & 0 \\ \sin\Theta & \cos\Theta & 0 \\ 0 & 0 & 1 \end{bmatrix}$$

where

$$\Theta - \arccos\left(\frac{y_{valve} - y_{apex}}{\sqrt{(x_{valve} - x_{apex})^2 + (y_{valve} - y_{apex})^2}}\right)$$

The rotation matrix for angle ϕ was defined as

$$R_\phi - \begin{bmatrix} 1 & 0 & 0 \\ 0 & \cos\Phi & \sin\Phi \\ 0 & -\sin\Phi & \cos\Phi \end{bmatrix}$$

where

$$\Phi - \arccos\left(\frac{z_{valve} - z_{apex}}{|n|}\right)$$

To rotate coordinate (x y z), I multiplied matrix R_ϕ by R_Θ, then multiplied their product by (x y z).

After the rotation, the markers were translated down the z axis until the base of the left ventricle was at the level of the origin. The amount of translation, z_{big}, was defined as the value of the largest z component (excluding the aortic valve markers).

$$\begin{bmatrix} x''_i \\ y''_i \\ z''_i \end{bmatrix} - \begin{bmatrix} x'_i \\ y'_i \\ z'_i \end{bmatrix} - \begin{bmatrix} 0 \\ 0 \\ z_{big} \end{bmatrix}$$

97

These translated and rotated coordinates were then used to fit the equation for an ellipsoid,

$$\frac{x^2}{a^2} + \frac{y^2}{b^2} + \frac{z^2}{c^2} = 1$$

In my model, a = b = semi-minor axis.

The equation for an ellipsoid can be linearized as follow. Let $x_1 = x^2$, $y_1 = y^2$, $z_1 = z^2$, $a_1 = 1/a^2$, $c_1 = 1/c^2$. The linearized equation is $a_1 (x_1 + y_1) + c_1 z_1 = 1$.

I used least squares regression to estimate the values of a_1 and c_1 from the coordinates of markers 1 through n, where n is the number of implanted markers. The marker coordinates were placed in a matrix A, the estimated semi-minor and semi-major axes were in the vector (a_0 c_0), and the least squares problem was defined as

$$\begin{bmatrix} (x_1(1)+y_1(1)) & z_1(1) \\ \cdot & \cdot \\ \cdot & \cdot \\ (x_1(n)+y_1(n)) & z_1(n) \end{bmatrix} \begin{bmatrix} a_0 \\ c_0 \end{bmatrix} = \begin{bmatrix} 1 \\ \cdot \\ \cdot \\ 1 \end{bmatrix}$$

or

$$A \begin{bmatrix} a_0 \\ c_0 \end{bmatrix} = b$$

The least squares solution to this problem is

$$\begin{bmatrix} a_0 \\ c_0 \end{bmatrix} = (A^T A)^{-1} A^T b$$

APPENDIX B

Computing Euler "Space-three" Angles

The following procedure from Kane et al. (33) was used to compute the Euler "space-three" angles, α_1, α_2, and α_3, from the orthonormal set of eigenvectors $E = [e_{ij}]$:

If the absolute value of E_{31} is not equal to 1, then let

$\alpha_2 = \text{arcsine} (-E_{31})$ where $-\pi/2 < \alpha_2 < \pi/2$.

Let $c_2 = \text{cosine } \alpha_2$, and let

$\beta_1 = \text{arcsine} (E_{32}/c_2)$ where $-\pi/2 \leq \beta_1 \leq \pi/2$

Then $\alpha_1 = \beta_1$ if $E_{33} \geq 0$, and $\alpha_1 = \pi - \beta_1$ if $E_{33} < 0$.

Let $\beta_3 = \text{arcsine} (E_{21}/c_2)$ where $-\pi/2 \leq \beta_3 \leq \pi/2$

and $\alpha_3 = \beta_3$ if $E_{11} \geq 0$, and $\alpha_3 = \pi - \beta_3$ if $E_{11} < 0$.

If the absolute value of $E_{31} = 1$, then let

$\alpha_2 = -\pi/2$ if $E_{31} = 1$, and $\alpha_1 = \pi/2$ if $E_{31} = -1$.

Define $\beta_1 = \text{arcsine} (-E_{23})$ $-\pi/2 \leq \beta_1 \leq \pi/2$ and let

$\alpha_1 = \beta_1$ if $E_{22} \geq 0$, and $\alpha_1 = \pi - \beta_1$ if $E_{22} < 0$

and define $\alpha_3 = 0$.